Simultaneous interval estimation of actuator fault and state for a class of nonlinear systems by zonotope analysis ☆

Chi Xu [a], Zhenhua Wang [a,*], Vicenç Puig [b], Yi Shen [a]

[a] Department of Control Science and Engineering, Harbin Institute of Technology, Harbin, 150001, PR China
[b] Advanced Control Systems (SAC) Research Group at Institut de Robòtica i Informàtica Industrial (IRI), CSIC-UPC, Automatic Control Department (ESAII), Universitat Politècnica de Catalunya-BarcelonaTech (UPC), Barcelona, Spain

A R T I C L E I N F O

Keywords:
Interval estimation
Fault estimation
Nonlinear systems
Zonotope analysis
Observer design

A B S T R A C T

In this paper, an actuator fault and state interval estimation method for a class of nonlinear systems is proposed by integrating observer design and zonotope analysis. For the considered systems, we present a novel unknown input observer structure with broad applications. The design procedure is based on H_∞ method to decrease the influence of unknown but bounded process disturbances and measurement noise. Moreover, a novel interval estimation method is presented based on zonotope analysis to obtain tighter intervals. Numerical simulations of a quadruple-tank system are conducted to assess the performance of the proposed approach.

1. Introduction

To enhance performance and product quality, industrial systems have become progressively complex, consequently escalating the likelihood of faults. To fulfill the requirements for reliability and safety, fault diagnosis schemes have received extensive attention in recent years [1–4]. As a part of the fault diagnosis scheme, rather than merely detecting fault occurrences, fault estimation methods aim to reconstruct faults and estimate their magnitudes. This estimation process plays a key role in implementing active fault-tolerant control (FTC) strategies [5–8].

In recent years, some results have been made in addressing the problem of fault estimation in nonlinear systems [9–11]. In [12], the authors presented a fault estimation method for Lipschitz nonlinear systems based on an intermediate estimator. State estimation and fault diagnosis method was designed by integrating optimal observer design and differential geometry for nonlinear systems subject to an actuator or plant fault [13]. However, the methods in [12,13] ignore the effect of measurement noise. To consider it, the authors of [14] addressed the fault estimation problem in the presence of unknown inputs and uncertain external disturbances. Their robust approach, formulated within the H_∞ framework, decouples the unknown input and attenuates the effect of external disturbances at the same time. [15] proposed a actuator fault estimation method based on delta operator and applied it to a two-stage chemical reactor system with time delays and external disturbances. In [16], the authors developed a new adaptive fuzzy observer design scheme to achieve fault estimation for a class of continuous-time nonlinear Markovian jump systems. However, these methods only focus on a punctual fault estimation but do not provide fault estimation uncertainty bounds.

Interval estimation provides a confidence interval for the estimated variables. The upper and lower bounds of the interval define the plausible range within which the true fault or state lies [17]. Interval estimation methods are mainly based on interval observers [18–22] and set-based interval estimation [23–25] methods. An unknown interval observer for discrete-time linear switched systems is presented in [19] which is based on the Input-to-State Stability. In [21], the authors proposed a T–N–L observer and applied it to the design of interval observers for discrete-time linear systems. By introducing parameter matrices $\boldsymbol{T}$ and $\boldsymbol{N}$, the T–N–L observer provides more design degrees of freedom. However, the design conditions of interval observers are often too strict to be satisfied, which limits their application range [23].

By combining an unknown input observer with a set-membership estimation technique, [26] addressed the joint state and fault estimation problem for a class of nonlinear systems affected by unknown bounded disturbance and actuator fault. The quadratic boundedness method is used to design the observer, and the interval estimation is obtained by overbounding the estimation error. Moreover, the uncertainties like disturbance and noise considered in [26] are assumed to be unknown bounded in ellipsoid sets. In [27], authors designed an ellipsoid-based framework for actuator fault estimation and the remaining useful life prediction. The actuator fault estimation is achieved by integrating L_∞ observer design and ellipsoid analysis. Similar to ellipsoids, zonotopes are a kind of geometric regions that provide a good trade-off

☆ This work was supported by the National Natural Science Foundation of China under Grant No. 62373125.
* Corresponding author.
E-mail address: zhenhua.wang@hit.edu.cn (Z. Wang).

between computational efficiency and estimation accuracy and have been widely used in the field of fault diagnosis [28–30]. A sensor fault estimation method for the discrete-time linear system is presented in [31], which transforms the system to an augmented descriptor system and uses the zonotopic Kalman filter to obtain the interval estimation. The authors of [32] proposed a fault detection method for nonlinear systems based on zonotopic filter, which demonstrates the potential of zonotopes in handling complex system dynamics. However, few joint fault and state interval estimation methods for discrete-time nonlinear systems have been designed, and it is still a challenging and worthwhile problem to be investigated.

Motivated by the above-mentioned discussion, this paper aims to propose a simultaneous actuator fault and state interval estimation approach for a class of nonlinear systems [14,26,33] by combining the observer design with zonotope analysis, and the considered systems are affected by unknown input and actuator fault. The main contributions are summarized as follows:

- An observer with a T–N–L structure is proposed to decouple the unknown input, and its sufficient design conditions are derived by using H_∞ method to minimize the influence of unknown but bounded disturbances and noise.
- Based on the proposed robust observer, zonotope analysis is used for fault and state interval estimation, obtaining tighter intervals than the existing method in [26].

This paper is organized as follows. Some preliminaries are given in Section 2. In Section 3, the interval estimation problem for a class of nonlinear systems is formulated. Section 4 presents the main results of the proposed method via a T–N–L observer design and zonotope analysis. In Section 5, numerical simulations under two fault scenarios are conducted to verify the effectiveness of the proposed method. Finally, the conclusions are drawn in Section 6.

2. Preliminaries

Notation: k is time step. $\mathbb{R}^n$ denotes n dimensional vector space, $\mathbb{R}^{n\times m}$ stand for the set of real matrices with $n \times m$ dimension. $\mathbb{R}^{\geq 0}$ represents the set of all non-negative real numbers. $\oplus$ is the symbol of Minkowski sum. The symbols $\leq$, $\geq$ and absolute value operator $|\cdot|$ are understood element-wise. For a vector $\boldsymbol{a} \in \mathbb{R}^n$, $\boldsymbol{a}(i)$ is the ith element of $\boldsymbol{a}$. $\text{diag}(\boldsymbol{a})$ denotes a diagonal matrix with $\boldsymbol{a}$ as the main diagonal. $\|\boldsymbol{a}\|_1 = \sum_{i=1}^{n} |\boldsymbol{a}(i)|$ denotes the L_1 norm of $\boldsymbol{a}$. The interval set $[\boldsymbol{a}] = [\boldsymbol{a}^-, \boldsymbol{a}^+]$ is introduced in Definition 1. For a matrix $\boldsymbol{A} \in \mathbb{R}^{n\times m}$, $\boldsymbol{A}^{\mathrm{T}}$ and $\boldsymbol{A}^{\dagger}$ are the transpose and pseudo-inverse matrix of $\boldsymbol{A}$, respectively. $\boldsymbol{A}(i,:)$ and $\boldsymbol{A}(i,j)$ represent the ith row vector and the (i,j)-th element in $\boldsymbol{A}$, respectively. The interval matrix set $[\boldsymbol{A}] = [\boldsymbol{A}^-, \boldsymbol{A}^+]$ is described in Definition 2. In a symmetric matrix, the asterisk $*$ stands for the symmetric term. $\boldsymbol{0}$ and $\boldsymbol{I}$ are zero and identity matrix, respectively. $\boldsymbol{P} \succ \boldsymbol{0}$ ($\boldsymbol{P} \prec \boldsymbol{0}$) presents that $\boldsymbol{P}$ is a positive (negative) definite square matrix. For a signal $\boldsymbol{x}$, $\|\boldsymbol{x}\|_2 = \sqrt{\sum_{k=1}^{\infty} \boldsymbol{x}_k^{\mathrm{T}} \boldsymbol{x}_k}$ denotes the L_2 normal of $\boldsymbol{x}$. $\alpha > 0$ ($\alpha < 0$) implies that α is positive (negative) scalar.

Definition 1. For a vector $\boldsymbol{a} \in \mathbb{R}^n$, the real interval vector $[\boldsymbol{a}] \subset \mathbb{R}^n$ is defined as:

$$[\boldsymbol{a}] = [\boldsymbol{a}^-, \boldsymbol{a}^+] = \left\{ \boldsymbol{a} \in \mathbb{R}^n : \boldsymbol{a}^- \leq \boldsymbol{a} \leq \boldsymbol{a}^+ \right\}. \tag{1}$$

where $\boldsymbol{a}^- \in \mathbb{R}^n, \boldsymbol{a}^+ \in \mathbb{R}^n$ are the lower and upper bound of $\boldsymbol{a}$, respectively.

Definition 2. For a matrix $\boldsymbol{A} \in \mathbb{R}^{n\times m}$, the real interval matrix $[\boldsymbol{A}] \subset \mathbb{R}^{n\times m}$ is defined as:

$$\begin{aligned}[\boldsymbol{A}] &= [\boldsymbol{A}^-, \boldsymbol{A}^+] \\ &= \left\{ \boldsymbol{A} \in \mathbb{R}^{n\times m} : \boldsymbol{A}^-(i,j) \leq \boldsymbol{A}(i,j) \leq \mathrm{A}^+(i,j)\,, \right. \\ &\quad \left. i = 1,\ldots,n, j = 1,\ldots,m \right\}.\end{aligned} \tag{2}$$

where $\boldsymbol{A}^- \in \mathbb{R}^{n\times m}, \boldsymbol{A}^+ \in \mathbb{R}^{n\times m}$ are the lower and upper bound of $\boldsymbol{A}$, respectively. The matrices $\boldsymbol{M}_{[\boldsymbol{A}]} \in \mathbb{R}^{n\times m}$, $\boldsymbol{R}_{[\boldsymbol{A}]} \in \mathbb{R}^{n\times m}$ and a vector $\boldsymbol{s}_{[\boldsymbol{A}]} \in \mathbb{R}^n$ associated with $[\boldsymbol{A}]$ are respectively defined as

$$\begin{aligned}\boldsymbol{M}_{[\boldsymbol{A}]} &= \frac{\boldsymbol{A}^+ + \boldsymbol{A}^-}{2}, \boldsymbol{R}_{[\boldsymbol{A}]} = \frac{\boldsymbol{A}^+ - \boldsymbol{A}^-}{2}, \\ \boldsymbol{s}_{[\boldsymbol{A}]} &= \sum_{j=1}^{m} \boldsymbol{R}_{[\boldsymbol{A}]}(i,j), i = 1,\ldots,n.\end{aligned} \tag{3}$$

Definition 3. An m-order zonotope $\mathcal{X} \subset \mathbb{R}^n$ is defined as:

$$\mathcal{X} = \boldsymbol{c} \oplus \boldsymbol{G}\mathcal{B}^m = \{\boldsymbol{c} + \boldsymbol{G}\varepsilon, \varepsilon \in \mathcal{B}^m\} \tag{4}$$

where $\boldsymbol{c} \in \mathbb{R}^n$ is the center of $\mathcal{X}$, $\boldsymbol{G} \in \mathbb{R}^{n\times m}$ is the generator matrix of $\mathcal{X}$, and $\mathcal{B}^m = [-1,1]^m$ is a hypercube. For simplicity, the zonotope is also denoted as $\mathcal{X} = \langle \boldsymbol{c}, \boldsymbol{G} \rangle$.

Property 1 (*[24]*). *The zonotopes in* $\mathbb{R}^n$ *satisfy:*

$$\langle \boldsymbol{c}_1, \boldsymbol{G}_1 \rangle \oplus \langle \boldsymbol{c}_2, \boldsymbol{G}_2 \rangle = \langle \boldsymbol{c}_1 + \boldsymbol{c}_2, [\boldsymbol{G}_1 \quad \boldsymbol{G}_2] \rangle \tag{5}$$

$$\boldsymbol{K}\langle \boldsymbol{c}, \boldsymbol{G} \rangle + \boldsymbol{a} = \langle \boldsymbol{K}\boldsymbol{c} + \boldsymbol{a}, \boldsymbol{K}\boldsymbol{G} \rangle \tag{6}$$

$$\mathcal{X} \in \langle \boldsymbol{c}, \boldsymbol{G} \rangle \subseteq \langle \boldsymbol{c}, \downarrow_d (\boldsymbol{G}) \rangle \tag{7}$$

$$\boldsymbol{x} \in \langle \boldsymbol{c}, \boldsymbol{G} \rangle \subseteq [\boldsymbol{x}] = [\boldsymbol{x}^-, \boldsymbol{x}^+] \tag{8}$$

where $\boldsymbol{K}$ *and* $\boldsymbol{a}$ *stand for the known matrix and vector with appropriate dimensions, respectively.* $\downarrow_d (\cdot)$ *is the zonotope reduction operator, where* $d(n < d < m)$ *is the chosen integer.* $\overline{\boldsymbol{G}}$ *denotes the matrix obtained by reordering the columns of* $\boldsymbol{G}$ *in decreasing Euclidean norm. Then,* $\downarrow_d (\boldsymbol{G}) = [\boldsymbol{G}^a, \boldsymbol{G}^b]$, $\boldsymbol{G}^a$ *is composed of the first* $d-n$ *columns of* $\overline{\boldsymbol{G}}$ *and* $\boldsymbol{G}^b$ *is a diagonal matrix with* $\boldsymbol{G}^b(i,i) = \sum_{j=d-n+1}^{m} \overline{\boldsymbol{G}}(i,j), i = 1,\ldots,n$. *Moreover, the bounds of* $\boldsymbol{x}$ *can be calculated as:*

$$\begin{cases} \boldsymbol{x}^-(i) = \boldsymbol{c}(i) - \|\boldsymbol{G}(i,:)\|_1 \\ \boldsymbol{x}^+(i) = \boldsymbol{c}(i) + \|\boldsymbol{G}(i,:)\|_1 \end{cases}, \quad i = 1,\ldots,n$$

Lemma 1 (*[21]*). *Given matrices* $\boldsymbol{Y} \in \mathbb{R}^{b\times c}$, $\boldsymbol{Z} \in \mathbb{R}^{a\times c}$, *if rank*$(\boldsymbol{Y}) = c$, *then the general solution of equation* $\boldsymbol{X}\boldsymbol{Y} = \boldsymbol{Z}$ *is obtained by*

$$\boldsymbol{X} = \boldsymbol{Z}\boldsymbol{Y}^{\dagger} + \boldsymbol{\Theta}(\boldsymbol{I}_c - \boldsymbol{Y}^{\dagger}\boldsymbol{Y}) \tag{9}$$

where $\boldsymbol{\Theta} \in \mathbb{R}^{a\times b}$ *is an arbitrary matrix.*

Lemma 2 (*[34]*). *There exist* $\boldsymbol{X} \succ \boldsymbol{0}, \boldsymbol{Y}$, $\boldsymbol{Z}$ *and* $\boldsymbol{O}$ *matrices with suitable dimension such that*

$$\boldsymbol{Z}^{\mathrm{T}}\boldsymbol{X}\boldsymbol{Z} - \boldsymbol{Y} \prec \boldsymbol{0} \tag{10}$$

$$\begin{bmatrix} -\boldsymbol{Y} & * \\ \boldsymbol{O}\boldsymbol{Z} & \boldsymbol{X} - \boldsymbol{O} - \boldsymbol{O}^{\mathrm{T}} \end{bmatrix} \prec \boldsymbol{0} \tag{11}$$

Lemma 3 (*Inclusion Function [35]*). *Let* $\boldsymbol{g} : \mathbb{R}^n \to \mathbb{R}^m$ *be a vector function, and* $[\boldsymbol{x}] \in \mathbb{R}^n$ *be an interval vector, the inclusion function* $[\boldsymbol{g}]$ *is defined as the application of* $\boldsymbol{g}$ *over the entire set represented by* $[\boldsymbol{x}]$, *that is*

$$\forall [\boldsymbol{x}] \in \mathbb{R}^n, \boldsymbol{g}([\boldsymbol{x}]) \subseteq [\boldsymbol{g}]([\boldsymbol{x}]) \tag{12}$$

where $[\boldsymbol{g}]$ *is derived by substituting each real variable with its corresponding interval and replacing standard operations with interval operations. The interval arithmetic operations are introduced in [36] and can be implemented using a toolbox as e.g. Cora [37].*

Lemma 4 (*Mean Value Extension [35]*). *Let* $\boldsymbol{g} : \mathbb{R}^n \to \mathbb{R}^m$ *be a nonlinear vector function with continuous first-order derivatives over a set* $\mathcal{X} \subseteq \mathbb{R}^n$. *For any real vector* $\boldsymbol{x} \in \mathcal{X}$, *the mean value extension of* $\boldsymbol{g}$ *over* $\mathcal{X}$ *can be expressed as*

$$\boldsymbol{g}(\mathcal{X}) \subseteq \boldsymbol{g}(\boldsymbol{x}) \oplus [\frac{\partial \boldsymbol{g}}{\partial \boldsymbol{x}}](\mathcal{X})(\mathcal{X} - \boldsymbol{x}) \tag{13}$$

where $[\frac{\partial \boldsymbol{g}}{\partial \boldsymbol{x}}](\mathcal{X})$ *denotes an interval enclosure for* $\frac{\partial \boldsymbol{g}}{\partial \boldsymbol{x}}$ *over* $\mathcal{X}$. *Moreover, using the zonotope to represent a set, i.e.,* $\mathcal{X} = \langle \boldsymbol{c}, \boldsymbol{G} \rangle \subseteq [\boldsymbol{x}]$, *(13) can be rewritten* as

$$g(\mathcal{X}) \subseteq g(\boldsymbol{c}) \oplus [\frac{\partial g}{\partial \boldsymbol{x}}]([\boldsymbol{x}])\langle \boldsymbol{0}, \boldsymbol{G}\rangle. \tag{14}$$

Lemma 5 (*Zonotope Inclusion [35]*). *Consider a family of zonotopes represented by $\mathcal{X} = \boldsymbol{c} \oplus [\boldsymbol{G}]\mathcal{B}^m$, where $\boldsymbol{c} \in \mathbb{R}^n$ is the center and $[\boldsymbol{G}] \in \mathbb{R}^{n\times m}$ is the interval generator matrix. The zonotope inclusion $\lozenge\mathcal{X}$ is defined by:*

$$\begin{aligned}\lozenge\mathcal{X} &= \boldsymbol{c} \oplus \left[\boldsymbol{M}_{[\boldsymbol{G}]}, \mathrm{diag}(\boldsymbol{s}_{[\boldsymbol{G}]})\right] \mathcal{B}^{m+n} \\ &= \langle \boldsymbol{c}, \left[\boldsymbol{M}_{[\boldsymbol{G}]}, \mathrm{diag}(\boldsymbol{s}_{[\boldsymbol{G}]})\right]\rangle \\ &= \langle \boldsymbol{c}, \mathrm{ZonIn}([\boldsymbol{G}])\rangle\end{aligned} \tag{15}$$

where $\boldsymbol{M}_{[\boldsymbol{G}]} \in \mathbb{R}^{n\times m}$, $\boldsymbol{s}_{[\boldsymbol{G}]}$ are a matrix and a vector related to $[\boldsymbol{G}]$ which can be computed by (3).

3. Problem formulation

Consider the following discrete-time nonlinear systems subject to unknown input disturbance and actuator fault

$$\begin{cases}\boldsymbol{x}_{k+1} = \boldsymbol{A}\boldsymbol{x}_k + \boldsymbol{B}\boldsymbol{u}_k + \boldsymbol{D}\boldsymbol{d}_k + \boldsymbol{h}(\boldsymbol{x}_k, \boldsymbol{u}_k) + \boldsymbol{B}\boldsymbol{f}_k + \boldsymbol{E}_1\boldsymbol{w}_k, \\ \boldsymbol{y}_k = \boldsymbol{C}\boldsymbol{x}_k + \boldsymbol{E}_2\boldsymbol{v}_k, \\ \boldsymbol{f}_{k+1} = \boldsymbol{f}_k + \boldsymbol{\Delta f}_k,\end{cases} \tag{16}$$

where $\boldsymbol{x}_k \in \mathbb{R}^{n_x}$ is the system state vector, $\boldsymbol{u}_k \in \mathbb{R}^{n_u}$ is the control input vector, $\boldsymbol{d}_k \in \mathbb{R}^{n_d}$ is the unknown input vector, $\boldsymbol{f}_k \in \mathbb{R}^{n_f}$ is the actuator fault vector, $\boldsymbol{y}_k \in \mathbb{R}^{n_y}$ is the measurement output vector, $\boldsymbol{w}_k \in \mathbb{R}^{n_w}$ is the process disturbance vector, $\boldsymbol{v}_k \in \mathbb{R}^{n_v}$ is the measurement noise vector, and $\boldsymbol{\Delta f}_k \in \mathbb{R}^{n_f}$ is the actuator fault variation. $\boldsymbol{A}, \boldsymbol{B}, \boldsymbol{C}, \boldsymbol{D}, \boldsymbol{F}, \boldsymbol{E}_1, \boldsymbol{E}_2$ are the known matrices with suitable dimensions. $\boldsymbol{h}(\boldsymbol{x}_k, \boldsymbol{u}_k)$ is a nonlinear vector function with first-order derivative with respect to $\boldsymbol{x}$. Based on the mean value theorem, we have

$$\boldsymbol{h}(\boldsymbol{a}, \boldsymbol{u}) - \boldsymbol{h}(\boldsymbol{b}, \boldsymbol{u}) = \boldsymbol{H}_{x,u}(\boldsymbol{a} - \boldsymbol{b}), \tag{17}$$

$$\boldsymbol{H}_{x,u} = \frac{\partial \boldsymbol{h}}{\partial \boldsymbol{x}}(\xi, \boldsymbol{u}) \in \mathbb{R}^{n\times n} \tag{18}$$

where $\xi \in [\boldsymbol{a}, \boldsymbol{b}], \xi \neq \boldsymbol{a}, \xi \neq \boldsymbol{b}$. According to the fact that state $\boldsymbol{x}$ is bounded, i.e., $\boldsymbol{x} \in [\boldsymbol{x}^-, \boldsymbol{x}^+]$, it can be obtained that

$$\boldsymbol{H}^- \leq \frac{\partial \boldsymbol{h}}{\partial \boldsymbol{x}}(\boldsymbol{x}, \boldsymbol{u}) \leq \boldsymbol{H}^+. \tag{19}$$

where $\boldsymbol{H}^-$, $\boldsymbol{H}^+$ are known matrix bounds. Based on Definition 2, $\boldsymbol{H}_{x,u} \in [\boldsymbol{H}] = [\boldsymbol{H}^-, \boldsymbol{H}^+]$ can be inferred.

In this paper, the following assumptions are considered.

Assumption 1. There exists a matrix $\boldsymbol{H} \in [\boldsymbol{H}]$, vectors $\boldsymbol{x}^- \leq \boldsymbol{a} < \boldsymbol{b} \leq \boldsymbol{x}^+$ and $\boldsymbol{\Delta h} = \boldsymbol{h}(\boldsymbol{a}, \boldsymbol{u}) - \boldsymbol{h}(\boldsymbol{b}, \boldsymbol{u})$, such that

$$\boldsymbol{\Delta h}^{\mathrm{T}}(\boldsymbol{a} - \boldsymbol{b}) \leq (\boldsymbol{a} - \boldsymbol{b})^{\mathrm{T}}\boldsymbol{H}^{\mathrm{T}}(\boldsymbol{a} - \boldsymbol{b}) \tag{20}$$

$$\boldsymbol{\Delta h}^{\mathrm{T}}\boldsymbol{\Delta h} \leq (\boldsymbol{a} - \boldsymbol{b})^{\mathrm{T}}\boldsymbol{H}^{\mathrm{T}}\boldsymbol{H}(\boldsymbol{a} - \boldsymbol{b}) \tag{21}$$

Notably, if $\boldsymbol{H}^{\mathrm{T}}\boldsymbol{H} = \gamma^2\boldsymbol{I}$, the condition in (21) aligns with the standard Lipschitz condition, with γ representing the Lipschitz constant. Moreover, if $\boldsymbol{H} = \rho\boldsymbol{I}$, the condition in (20) aligns with the one-sided Lipschitz condition. Consequently, the proposed method in this paper accommodates a broader range of systems.

Assumption 2. To decouple the effects of unknown inputs, the following rank condition needs to be satisfied as

$$\mathrm{rank}(\boldsymbol{C}\boldsymbol{D}) = \mathrm{rank}(\boldsymbol{D}) = n_d, n_d < n_y \tag{22}$$

Assumption 3. The initial state $\boldsymbol{x}_0$, the initial fault $\boldsymbol{f}_0$, the process disturbance $\boldsymbol{w}_k$, the measurement noise $\boldsymbol{v}_k$ and the actuator fault variation $\boldsymbol{\Delta f}_k$ in system (16) are assumed to be unknown but bounded as follows:

$$\begin{aligned}&|\boldsymbol{x}_0 - \boldsymbol{c}_{x,0}| \leq \tilde{\boldsymbol{x}}, \quad |\boldsymbol{f}_0 - \boldsymbol{c}_{f,0}| \leq \tilde{\boldsymbol{f}}, \quad |\boldsymbol{w}_k| \leq \tilde{\boldsymbol{w}}, \\ &|\boldsymbol{v}_k| \leq \tilde{\boldsymbol{v}}, \quad |\boldsymbol{\Delta f}_k| \leq \boldsymbol{\Delta}\tilde{\boldsymbol{f}},\end{aligned} \tag{23}$$

where $\tilde{\boldsymbol{x}}, \tilde{\boldsymbol{w}}, \tilde{\boldsymbol{v}}$, and $\boldsymbol{\Delta}\tilde{\boldsymbol{f}}$ are known vectors.

Remark 1. If Assumption 2 does not hold, the effects of unknown input cannot be fully decoupled, but can be mitigated. If Assumption 3 is not met, the results obtained by the set-membership estimation method are overly conservative due to the lack of boundary assumptions. Although this could reduce precision and reliability, these methods may still useful.

This paper aims to design an interval estimation method to find both actuator fault interval $[\boldsymbol{f}_k]$ and state interval $[\boldsymbol{x}_k]$ such that $\boldsymbol{f}_k^- \leq \boldsymbol{f}_k \leq \boldsymbol{f}_k^+$ and $\boldsymbol{x}_k^- \leq \boldsymbol{x}_k \leq \boldsymbol{x}_k^+$, instead of a single point estimation, providing these intervals tighter as possible.

4. Simultaneous interval estimation of state and actuator fault

In this section, a robust observer and its sufficient design conditions will be presented. Then, an interval estimation of the state and actuator fault method based on zonotope analysis is provided.

4.1. A T–N–L observer design

A robust observer with T–N–L structure is proposed for system (16):

$$\begin{cases}\hat{\boldsymbol{z}}_{k+1} = \boldsymbol{T}\boldsymbol{A}\hat{\boldsymbol{x}}_k + \boldsymbol{T}\boldsymbol{B}\boldsymbol{u}_k + \boldsymbol{T}\boldsymbol{h}(\hat{\boldsymbol{x}}_k, \boldsymbol{u}_k) + \boldsymbol{T}\boldsymbol{B}\hat{\boldsymbol{f}}_k \\ \qquad + \boldsymbol{L}_1(\boldsymbol{y}_k - \boldsymbol{C}\hat{\boldsymbol{x}}_k) \\ \hat{\boldsymbol{x}}_k = \hat{\boldsymbol{z}}_k + \boldsymbol{N}\boldsymbol{y}_k \\ \hat{\boldsymbol{f}}_{k+1} = \hat{\boldsymbol{f}}_k + \boldsymbol{L}_2(\boldsymbol{y}_k - \boldsymbol{C}\hat{\boldsymbol{x}}_k)\end{cases} \tag{24}$$

where $\hat{\boldsymbol{z}}_k \in \mathbb{R}^{n_x}$, $\hat{\boldsymbol{x}}_k \in \mathbb{R}^{n_x}$, $\hat{\boldsymbol{f}}_k \in \mathbb{R}^{n_f}$ denote the observer intermediate state, the estimate of $\boldsymbol{x}_k$ and the estimate of $\boldsymbol{f}_k$, respectively. $\boldsymbol{T} \in \mathbb{R}^{n_x\times n_x}$, $\boldsymbol{N} \in \mathbb{R}^{n_y\times n_x}$, $\boldsymbol{L}_1 \in \mathbb{R}^{n_x\times n_y}$, $\boldsymbol{L}_2 \in \mathbb{R}^{n_f\times n_y}$ are parameter matrices that should be designed. In addition, $\boldsymbol{T}$ and $\boldsymbol{N}$ need to satisfy the following relations:

$$\boldsymbol{T}\boldsymbol{D} = \boldsymbol{0}, \tag{25}$$

$$\boldsymbol{T} + \boldsymbol{N}\boldsymbol{C} = \boldsymbol{I}_{n_x}. \tag{26}$$

$\boldsymbol{T}$ and $\boldsymbol{N}$ can be considered as weighting matrices to select information from model and measurement outputs. (25) ensures that unknown input $\boldsymbol{d}_k$ does not affect the state estimation. By post-multiplying (26) with $\boldsymbol{D}$, we get

$$\boldsymbol{N}\boldsymbol{C}\boldsymbol{D} = \boldsymbol{D}. \tag{27}$$

Based on Assumption 1 and Lemma 1, the general solution of $\boldsymbol{N}$ and $\boldsymbol{T}$ can be obtained as

$$\boldsymbol{N} = \boldsymbol{D}(\boldsymbol{C}\boldsymbol{D})^{\dagger} + \boldsymbol{\Theta}(\boldsymbol{I}_{n_y} - (\boldsymbol{C}\boldsymbol{D})(\boldsymbol{C}\boldsymbol{D})^{\dagger}) \tag{28}$$

$$\boldsymbol{T} = \boldsymbol{I}_{n_x} - \boldsymbol{D}(\boldsymbol{C}\boldsymbol{D})^{\dagger}\boldsymbol{C} - \boldsymbol{\Theta}(\boldsymbol{I}_{n_y} - (\boldsymbol{C}\boldsymbol{D})(\boldsymbol{C}\boldsymbol{D})^{\dagger})\boldsymbol{C} \tag{29}$$

where $\boldsymbol{\Theta} \in \mathbb{R}^{n_x\times n_y}$ is an arbitrary matrix that need to be determined.

To analyze observer (24), the state and fault estimation error is defined as

$$\boldsymbol{e}_{x,k} = \boldsymbol{x}_k - \hat{\boldsymbol{x}}_k, \tag{30}$$

$$\boldsymbol{e}_{f,k} = \boldsymbol{f}_k - \hat{\boldsymbol{f}}_k. \tag{31}$$

Taking into account (16), (24)–(26), we have:

$$\begin{aligned}\boldsymbol{e}_{x,k+1} &= (\boldsymbol{T} + \boldsymbol{N}\boldsymbol{C})\boldsymbol{x}_{k+1} - \hat{\boldsymbol{z}}_{k+1} - \boldsymbol{N}\boldsymbol{y}_{k+1} \\ &= \boldsymbol{T}\boldsymbol{x}_{k+1} + \boldsymbol{N}(\boldsymbol{y}_{k+1} - \boldsymbol{E}_2\boldsymbol{v}_{k+1}) - \hat{\boldsymbol{z}}_{k+1} - \boldsymbol{N}\boldsymbol{y}_{k+1} \\ &= (\boldsymbol{T}\boldsymbol{A} - \boldsymbol{L}_1\boldsymbol{C})\boldsymbol{e}_{x,k} + \boldsymbol{T}\boldsymbol{B}\boldsymbol{e}_{f,k} \\ &\quad - \boldsymbol{T}(\boldsymbol{h}(\boldsymbol{x}_k, \boldsymbol{u}_k) - \boldsymbol{h}(\hat{\boldsymbol{x}}_k, \boldsymbol{u}_k)) \\ &\quad + \boldsymbol{T}\boldsymbol{E}_1\boldsymbol{w}_k - \boldsymbol{L}_1\boldsymbol{E}_2\boldsymbol{v}_k - \boldsymbol{N}\boldsymbol{E}_2\boldsymbol{v}_{k+1}\end{aligned} \tag{32}$$

$$\begin{aligned}\boldsymbol{e}_{f,k+1} &= \boldsymbol{f}_k + \boldsymbol{\Delta f}_k - \hat{\boldsymbol{f}}_k - \boldsymbol{L}_2(\boldsymbol{y}_k - \boldsymbol{C}\hat{\boldsymbol{x}}_k) \\ &= \boldsymbol{L}_2\boldsymbol{C}\boldsymbol{e}_{x,k} + \boldsymbol{e}_{f,k} + \boldsymbol{\Delta f}_k - \boldsymbol{L}_2\boldsymbol{E}_2\boldsymbol{v}_k.\end{aligned} \tag{33}$$

By defining

$$\bar{e}_k = \begin{bmatrix} e_{x,k} \\ e_{f,k} \end{bmatrix}, \boldsymbol{\Delta h}_k = \boldsymbol{h}(\boldsymbol{x}_k, \boldsymbol{u}_k) - \boldsymbol{h}(\hat{\boldsymbol{x}}_k, \boldsymbol{u}_k), \bar{\boldsymbol{w}}_k = \begin{bmatrix} \boldsymbol{w}_k \\ \boldsymbol{\Delta f}_k \\ \boldsymbol{v}_k \\ \boldsymbol{v}_{k+1} \end{bmatrix}, \tag{34}$$

the augmented error dynamic system can be formulated as

$$\bar{e}_{k+1} = \boldsymbol{S}\bar{e}_k + \bar{\boldsymbol{T}}\boldsymbol{\Delta h}_k + \bar{\boldsymbol{E}}\bar{\boldsymbol{w}}_k \tag{35}$$

where

$$\begin{aligned} &\boldsymbol{S} = \bar{\boldsymbol{A}} - \bar{\boldsymbol{L}}\bar{\boldsymbol{C}}, \bar{\boldsymbol{E}} = \bar{\boldsymbol{E}}_1 - \bar{\boldsymbol{L}}\bar{\boldsymbol{E}}_2, \bar{\boldsymbol{A}} = \begin{bmatrix} \boldsymbol{TA} & \boldsymbol{TB} \\ \boldsymbol{0} & \boldsymbol{I} \end{bmatrix}, \\ &\bar{\boldsymbol{L}} = \begin{bmatrix} \boldsymbol{L}_1 \\ \boldsymbol{L}_2 \end{bmatrix}, \bar{\boldsymbol{E}}_1 = \begin{bmatrix} \boldsymbol{TE}_1 & \boldsymbol{0} & \boldsymbol{0} & -\boldsymbol{NE}_2 \\ \boldsymbol{0} & \boldsymbol{I} & \boldsymbol{0} & \boldsymbol{0} \end{bmatrix}, \\ &\bar{\boldsymbol{E}}_2 = \begin{bmatrix} \boldsymbol{0} & \boldsymbol{0} & \boldsymbol{E}_2 & \boldsymbol{0} \end{bmatrix}, \bar{\boldsymbol{C}} = \begin{bmatrix} \boldsymbol{C} & \boldsymbol{0} \end{bmatrix}. \end{aligned} \tag{36}$$

Based on the augmented error dynamic system (35), the following theorem is proposed to give sufficient design conditions for fault and state observer (24).

Theorem 1. *For a prescribed* $\bar{\boldsymbol{w}}_k \in \mathbb{R}^{n_{\bar{\omega}}}$ $(n_{\bar{\omega}} = n_x + n_f + 2n_v)$ *attenuation level* $\delta > 0$*, if there exist constants* $\alpha > 0$*,* $\beta > 0$*, matrices* $\boldsymbol{P} \succ \boldsymbol{0} \in \mathbb{R}^{(n_x+n_f)\times(n_x+n_f)}$*,* $\boldsymbol{W} \in \mathbb{R}^{(n_x+n_f)\times n_y}$ *and* $\boldsymbol{O} \in \mathbb{R}^{n_x\times n_x}$ *for all* $\boldsymbol{H} \in [\boldsymbol{H}]$ *such that*

$$\begin{bmatrix} \boldsymbol{\Gamma}_{11} & * & * & * & * \\ -\alpha\boldsymbol{Y} & -\beta\boldsymbol{I}_{n_x} & * & * & * \\ \boldsymbol{0} & \boldsymbol{0} & -\delta^2\boldsymbol{I}_{n_{\bar{\omega}}} & * & * \\ \boldsymbol{P}\bar{\boldsymbol{A}} - \boldsymbol{W}\bar{\boldsymbol{C}} & \boldsymbol{P}\bar{\boldsymbol{T}} & \boldsymbol{P}\bar{\boldsymbol{E}}_1 - \boldsymbol{W}\bar{\boldsymbol{E}}_2 & -\boldsymbol{P} & * \\ \boldsymbol{OHY} & \boldsymbol{0} & \boldsymbol{0} & \boldsymbol{0} & \boldsymbol{\Gamma}_{55} \end{bmatrix} \prec \boldsymbol{0} \tag{37}$$

where

$$\boldsymbol{\Gamma}_{11} = \boldsymbol{I}_{n_x+n_f} - \boldsymbol{P} + \alpha\boldsymbol{Y}^{\mathrm{T}}(\boldsymbol{H}^{\mathrm{T}} + \boldsymbol{H})\boldsymbol{Y},$$

$$\boldsymbol{\Gamma}_{55} = \beta\boldsymbol{I}_{n_x} - \boldsymbol{O} - \boldsymbol{O}^{\mathrm{T}},$$

$$\boldsymbol{Y} = [\boldsymbol{I}_{n_x} \quad \boldsymbol{0}].$$

Then, the augmented error system in (35) *is stable and satisfies the condition*

$$(\|\bar{e}\|_2)^2 \le \delta^2(\|\bar{\boldsymbol{w}}\|_2)^2 + \bar{e}_0^{\mathrm{T}}\boldsymbol{P}\bar{e}_0. \tag{38}$$

To improve estimation performance, the following optimization problem needs to be solved

$$\min \quad \delta^2, \quad \text{s.t. } (37). \tag{39}$$

Then, if the optimization problem in (39) *is solvable, the matrices* $\boldsymbol{L}_1$ *and* $\boldsymbol{L}_2$ *can be determined by*

$$\begin{aligned} &\bar{\boldsymbol{L}} = \boldsymbol{P}^{-1}\boldsymbol{W}, \boldsymbol{L}_1 = \bar{\boldsymbol{L}}(1:n_x,:), \\ &\boldsymbol{L}_2 = \bar{\boldsymbol{L}}(n_x+1:n_x+n_f,:). \end{aligned} \tag{40}$$

Proof. The following Lyapunov function for the augmented system is defined as:

$$V_k = \bar{e}_k^{\mathrm{T}}\boldsymbol{P}\bar{e}_k, \quad \boldsymbol{P} \succ \boldsymbol{0} \tag{41}$$

and its time difference is

$$\Delta V_k = V_{k+1} - V_k = \bar{e}_{k+1}^{\mathrm{T}}\boldsymbol{P}\bar{e}_{k+1} - \bar{e}_k^{\mathrm{T}}\boldsymbol{P}\bar{e}_k. \tag{42}$$

Substituting (35) into (42) yields

$$\Delta V_k = [\bar{e}_k^{\mathrm{T}} \quad \boldsymbol{\Delta h}_k^{\mathrm{T}} \quad \bar{\boldsymbol{w}}_k^{\mathrm{T}}]\boldsymbol{\Psi}[\bar{e}_k^{\mathrm{T}} \quad \boldsymbol{\Delta h}_k^{\mathrm{T}} \quad \bar{\boldsymbol{w}}_k^{\mathrm{T}}]^{\mathrm{T}} \tag{43}$$

with

$$\boldsymbol{\Psi} = \begin{bmatrix} \boldsymbol{S}^{\mathrm{T}}\boldsymbol{PS} & * & * \\ \bar{\boldsymbol{T}}^{\mathrm{T}}\boldsymbol{PS} & \bar{\boldsymbol{T}}^{\mathrm{T}}\boldsymbol{P}\bar{\boldsymbol{T}} & * \\ \bar{\boldsymbol{E}}^{\mathrm{T}}\boldsymbol{PS} & \bar{\boldsymbol{E}}^{\mathrm{T}}\boldsymbol{P}\bar{\boldsymbol{T}} & \bar{\boldsymbol{E}}^{\mathrm{T}}\boldsymbol{P}\bar{\boldsymbol{E}} \end{bmatrix}. \tag{44}$$

Substituting

$$\boldsymbol{PS} = \boldsymbol{P}\bar{\boldsymbol{A}} - \boldsymbol{P}\bar{\boldsymbol{L}}\bar{\boldsymbol{C}} = \boldsymbol{P}\bar{\boldsymbol{A}} - \boldsymbol{W}\bar{\boldsymbol{C}},$$

$$\boldsymbol{P}\bar{\boldsymbol{E}} = \boldsymbol{P}\bar{\boldsymbol{E}}_1 - \boldsymbol{P}\bar{\boldsymbol{L}}\bar{\boldsymbol{E}}_2 = \boldsymbol{P}\bar{\boldsymbol{E}}_1 - \boldsymbol{W}\bar{\boldsymbol{E}}_2,$$

with $\boldsymbol{W} = \boldsymbol{P}\bar{\boldsymbol{L}}$ into (37), inequality (37) becomes

$$\begin{bmatrix} \boldsymbol{\Gamma}_{11} & * & * & * & * \\ -\alpha\boldsymbol{Y} & -\beta\boldsymbol{I}_{n_x} & * & * & * \\ \boldsymbol{0} & \boldsymbol{0} & -\delta^2\boldsymbol{I}_{n_{\bar{\omega}}} & * & * \\ \boldsymbol{PS} & \boldsymbol{P}\bar{\boldsymbol{T}} & \boldsymbol{P}\bar{\boldsymbol{E}} & -\boldsymbol{P} & * \\ \boldsymbol{OHY} & \boldsymbol{0} & \boldsymbol{0} & \boldsymbol{0} & \boldsymbol{\Gamma}_{55} \end{bmatrix} \prec \boldsymbol{0}. \tag{45}$$

Taking into account Lemma 2, (45) can be rewritten as

$$\begin{bmatrix} \boldsymbol{\Upsilon}_{11} & * & * & * \\ -\alpha\boldsymbol{Y} & -\beta\boldsymbol{I}_{n_x} & * & * \\ \boldsymbol{0} & \boldsymbol{0} & -\delta^2\boldsymbol{I}_{n_{\bar{\omega}}} & * \\ \boldsymbol{PS} & \boldsymbol{P}\bar{\boldsymbol{T}} & \boldsymbol{P}\bar{\boldsymbol{E}} & -\boldsymbol{P} \end{bmatrix} \prec \boldsymbol{0}. \tag{46}$$

where $\boldsymbol{\Upsilon}_{11} = \boldsymbol{I}_{n_x+n_f} - \boldsymbol{P} + \alpha\boldsymbol{Y}^{\mathrm{T}}(\boldsymbol{H}^{\mathrm{T}} + \boldsymbol{H})\boldsymbol{Y} + \beta\boldsymbol{Y}^{\mathrm{T}}\boldsymbol{H}^{\mathrm{T}}\boldsymbol{HY}$.

Then, we apply the Schur complement lemma [38] to rewrite (46) as

$$\begin{bmatrix} \boldsymbol{\Xi}_{11} & * & * \\ \bar{\boldsymbol{T}}^{\mathrm{T}}\boldsymbol{PS} - \alpha\boldsymbol{Y} & \bar{\boldsymbol{T}}^{\mathrm{T}}\boldsymbol{P}\bar{\boldsymbol{T}} - \beta\boldsymbol{I}_{n_x} & * \\ \bar{\boldsymbol{E}}^{\mathrm{T}}\boldsymbol{PS} & \bar{\boldsymbol{E}}^{\mathrm{T}}\boldsymbol{P}\bar{\boldsymbol{T}} & \boldsymbol{\Xi}_{33} \end{bmatrix} \prec \boldsymbol{0}, \tag{47}$$

with $\boldsymbol{\Xi}_{11} = \boldsymbol{S}^{\mathrm{T}}\boldsymbol{PS} + \boldsymbol{I}_{n_x+n_f} - \boldsymbol{P} + \alpha\boldsymbol{Y}^{\mathrm{T}}(\boldsymbol{H}^{\mathrm{T}} + \boldsymbol{H})\boldsymbol{Y} + \beta\boldsymbol{Y}^{\mathrm{T}}\boldsymbol{H}^{\mathrm{T}}\boldsymbol{HY}$, $\boldsymbol{\Xi}_{33} = \bar{\boldsymbol{E}}^{\mathrm{T}}\boldsymbol{P}\bar{\boldsymbol{E}} - \delta^2\boldsymbol{I}_{n_{\bar{\omega}}}$, and it equals to

$$\boldsymbol{\Psi} + \begin{bmatrix} \boldsymbol{\Upsilon}_{11} & * & * \\ -\alpha\boldsymbol{Y} & -\beta\boldsymbol{I}_{n_x} & * \\ \boldsymbol{0} & \boldsymbol{0} & -\delta^2\boldsymbol{I}_{n_{\bar{\omega}}} \end{bmatrix} \prec \boldsymbol{0}, \tag{48}$$

Now, we can get that if (48) is satisfied, (37) holds.

Pre- and post-multiplying (48) with $[\bar{e}_k^{\mathrm{T}} \quad \boldsymbol{\Delta h}_k^{\mathrm{T}} \quad \bar{\boldsymbol{w}}_k^{\mathrm{T}}]$ and its transpose, respectively. we obtain that

$$\Delta V_k + \bar{e}_k^{\mathrm{T}}\bar{e}_k - \delta^2\bar{\boldsymbol{w}}_k^{\mathrm{T}}\bar{\boldsymbol{w}}_k + \mu_1 + \mu_2 \le 0. \tag{49}$$

where $\mu_1 = \alpha\bar{e}_k^{\mathrm{T}}\boldsymbol{Y}^{\mathrm{T}}(\boldsymbol{H}^{\mathrm{T}} + \boldsymbol{H})\boldsymbol{Y}\bar{e}_k - \alpha\boldsymbol{\Delta h}_k^{\mathrm{T}}\boldsymbol{Y}\bar{e}_k - \alpha\bar{e}_k^{\mathrm{T}}\boldsymbol{Y}^{\mathrm{T}}\boldsymbol{\Delta h}_k$, $\mu_2 = \beta\bar{e}_k^{\mathrm{T}}\boldsymbol{Y}^{\mathrm{T}}\boldsymbol{H}^{\mathrm{T}}\boldsymbol{HY}\bar{e}_k - \beta\boldsymbol{\Delta h}_k^{\mathrm{T}}\boldsymbol{\Delta h}_k$.

According to (20) in Assumption 1, we have

$$\begin{aligned} \boldsymbol{\Delta h}_k^{\mathrm{T}}(\boldsymbol{x}_k - \hat{\boldsymbol{x}}_k) &\le (\boldsymbol{x}_k - \hat{\boldsymbol{x}}_k)^{\mathrm{T}}\boldsymbol{H}^{\mathrm{T}}(\boldsymbol{x}_k - \hat{\boldsymbol{x}}_k) \\ \boldsymbol{\Delta h}_k^{\mathrm{T}}e_{x,k} &\le e_{x,k}^{\mathrm{T}}\boldsymbol{H}^{\mathrm{T}}e_{x,k} \\ \boldsymbol{\Delta h}_k^{\mathrm{T}}e_{x,k} &\le \frac{1}{2}e_{x,k}^{\mathrm{T}}(\boldsymbol{H}^{\mathrm{T}} + \boldsymbol{H})e_{x,k} \end{aligned}$$

$$\boldsymbol{\Delta h}_k^{\mathrm{T}}e_{x,k} + e_{x,k}^{\mathrm{T}}\boldsymbol{\Delta h}_k \le e_{x,k}^{\mathrm{T}}(\boldsymbol{H}^{\mathrm{T}} + \boldsymbol{H})e_{x,k}. \tag{50}$$

Based on (34), it follows

$$e_{x,k} = [\boldsymbol{I}_{n_x} \quad \boldsymbol{0}]\begin{bmatrix} e_{x,k} \\ e_{f,k} \end{bmatrix} = \boldsymbol{Y}\bar{e}_k \tag{51}$$

Substituting (51) into (50) yields that

$$\boldsymbol{\Delta h}_k^{\mathrm{T}}\boldsymbol{Y}\bar{e}_k + \bar{e}_k^{\mathrm{T}}\boldsymbol{Y}^{\mathrm{T}}\boldsymbol{\Delta h}_k \le \bar{e}_k^{\mathrm{T}}\boldsymbol{Y}^{\mathrm{T}}(\boldsymbol{H}^{\mathrm{T}} + \boldsymbol{H})\boldsymbol{Y}\bar{e}_k$$

$$\bar{e}_k^{\mathrm{T}}\boldsymbol{Y}^{\mathrm{T}}(\boldsymbol{H}^{\mathrm{T}} + \boldsymbol{H})\boldsymbol{Y}\bar{e}_k - \boldsymbol{\Delta h}_k^{\mathrm{T}}\boldsymbol{Y}\bar{e}_k - \bar{e}_k^{\mathrm{T}}\boldsymbol{Y}^{\mathrm{T}}\boldsymbol{\Delta h}_k \ge 0 \tag{52}$$

Similarly, based on (21) in Assumption 1, we obtain

$$\begin{aligned} \boldsymbol{\Delta h}_k^{\mathrm{T}}\boldsymbol{\Delta h}_k &\le (\boldsymbol{x}_k - \hat{\boldsymbol{x}}_k)^{\mathrm{T}}\boldsymbol{H}^{\mathrm{T}}\boldsymbol{H}(\boldsymbol{x}_k - \hat{\boldsymbol{x}}_k) \\ \boldsymbol{\Delta h}_k^{\mathrm{T}}\boldsymbol{\Delta h}_k &\le e_{x,k}^{\mathrm{T}}\boldsymbol{H}^{\mathrm{T}}\boldsymbol{H}e_{x,k} \\ \boldsymbol{\Delta h}_k^{\mathrm{T}}\boldsymbol{\Delta h}_k &\le \bar{e}_k^{\mathrm{T}}\boldsymbol{Y}^{\mathrm{T}}\boldsymbol{H}^{\mathrm{T}}\boldsymbol{HY}\bar{e}_k \end{aligned}$$

$$\bar{e}_k^{\mathrm{T}}\boldsymbol{Y}^{\mathrm{T}}\boldsymbol{H}^{\mathrm{T}}\boldsymbol{HY}\bar{e}_k - \boldsymbol{\Delta h}_k^{\mathrm{T}}\boldsymbol{\Delta h}_k \ge 0. \tag{53}$$

Substituting (52), (53) into (49) yields

$$\Delta V_k + \bar{e}_k^{\mathrm{T}}\bar{e}_k - \delta^2\bar{\boldsymbol{w}}_k^{\mathrm{T}}\bar{\boldsymbol{w}}_k \le 0 \tag{54}$$

When $\boldsymbol{w}_k = \boldsymbol{0}$, we have

$$\Delta V_k \leq -\boldsymbol{e}_k^{\mathrm{T}} \boldsymbol{e}_k \leq 0 \tag{55}$$

which implies the augmented error system in (35) is stable.

Then, we define a criterion as

$$J = \sum_{k=1}^{\infty} (\Delta V_k + \bar{\boldsymbol{e}}_k^{\mathrm{T}} \bar{\boldsymbol{e}}_k - \delta^2 \overline{\boldsymbol{w}}_k^{\mathrm{T}} \overline{\boldsymbol{w}}_k). \tag{56}$$

According to (42), (56) becomes

$$J = V_\infty - V_0 + \sum_{k=1}^{\infty} (\bar{\boldsymbol{e}}_k^{\mathrm{T}} \bar{\boldsymbol{e}}_k - \delta^2 \overline{\boldsymbol{w}}_k^{\mathrm{T}} \overline{\boldsymbol{w}}_k). \tag{57}$$

It is evident that if (54) holds, $J < 0$. Due to $\boldsymbol{P} > \boldsymbol{0}$, we have $V_\infty \geq 0$. (57) equals to $(\|\bar{\boldsymbol{e}}\|_2)^2 - \delta^2 (\|\overline{\boldsymbol{w}}\|_2)^2 - V_0 = J - V_\infty$. Then $J < 0$ implies $(\|\bar{\boldsymbol{e}}\|_2)^2 - \delta^2 (\|\overline{\boldsymbol{w}}\|_2)^2 - V_0 \leq 0$ and (38) holds. The optimization problem in (45) should be solved for obtaining an accurate interval estimation of $\boldsymbol{f}_k$ and $\boldsymbol{x}_k$. Additionally, considering the relations in (36), the required parameter matrices $\boldsymbol{L}_1$ and $\boldsymbol{L}_2$ can be obtained by (40). □

Remark 2. The interval matrix $[\boldsymbol{H}] = [\boldsymbol{H}^-, \boldsymbol{H}^+] \in \mathbb{R}^n$ in Definition 2 can be equivalently expressed as

$$[\boldsymbol{H}] = \left\{ \boldsymbol{H}(\lambda) : \boldsymbol{H}(\lambda) = \sum_{i=1}^{\eta} \lambda(i) \boldsymbol{H}_i, \sum_{i=1}^{\eta} \lambda(i) = 1, \right.$$
$$\left. \lambda(i) \geq 0, \quad \eta = 2^{n^2} \right\} \tag{58}$$

where $\boldsymbol{H}_i$ is a matrix composed by the elements of $\boldsymbol{H}^-$ and $\boldsymbol{H}^+$, i.e. $\boldsymbol{H}_i(j_1, j_2) = \{\boldsymbol{H}^-(j_1, j_2), \boldsymbol{H}^+(j_1, j_2)\}$, $j_1, j_2 = 1, \ldots, \eta$. Considering there are constant elements in $\boldsymbol{H}$, η can be calculated by $\eta = 2^{n^2 - \phi}$ with ϕ is the number of constant elements in $\boldsymbol{H}$. Therefore, substituting (58) to (37) and applying S-procedure, the uncertainty problem in (37) is transformed into a semi-definite programming problem. Similar processing procedures have been applied in existing research [14,26] and theoretically ensures the conservativeness and feasibility of the results. Solving (37) is equivalent to solving

For $\quad i = 1, \ldots, \eta$

$$\begin{bmatrix} \boldsymbol{\Gamma}_{11}(i) & * & * & * & * \\ -\alpha \boldsymbol{Y} & -\beta \boldsymbol{I}_{n_x} & * & * & * \\ \boldsymbol{0} & \boldsymbol{0} & -\delta^2 \boldsymbol{I}_{n_{\overline{\omega}}} & * & * \\ \boldsymbol{P}\overline{\boldsymbol{A}} - \boldsymbol{W}\overline{\boldsymbol{C}} & \boldsymbol{P}\overline{\boldsymbol{T}} & \boldsymbol{P}\overline{\boldsymbol{E}}_1 - \boldsymbol{W}\overline{\boldsymbol{E}}_2 & -\boldsymbol{P} & * \\ \boldsymbol{O}\boldsymbol{H}_{i\boldsymbol{Y}} & \boldsymbol{0} & \boldsymbol{0} & \boldsymbol{0} & \boldsymbol{\Gamma}_{55} \end{bmatrix} < \boldsymbol{0} \tag{59}$$

with $\boldsymbol{\Gamma}_{11}(i) = \boldsymbol{I}_{n_x + n_f} - \boldsymbol{P} + \alpha \boldsymbol{Y}^{\mathrm{T}} (\boldsymbol{H}_i^{\mathrm{T}} + \boldsymbol{H}_i) \boldsymbol{Y}$. Correspondingly, the optimization problem in (38) becomes

$$\min \quad \delta^2, \quad \text{s.t. (59)}. \tag{60}$$

4.2. Zonotope-based interval estimation

After determining the observer (24), the zonotope analysis is used to achieve the state and actuator fault interval estimation for the system in (16) by means of the following theorem.

Theorem 2. *Given $\boldsymbol{x}_0 \in \mathcal{X}_{x,0} = \langle \boldsymbol{c}_{x,0}, \boldsymbol{G}_{x,0} \rangle$, $\boldsymbol{f}_0 \in \mathcal{X}_{f,0} = \langle \boldsymbol{c}_{f,0}, \boldsymbol{G}_{f,0} \rangle$, $\hat{\boldsymbol{x}}_0 = \boldsymbol{c}_{x,0}$ and $\hat{\boldsymbol{f}}_0 = \boldsymbol{c}_{f,0}$, the initial augmented error $\bar{\boldsymbol{e}}_0$ is defined as*

$$\bar{\boldsymbol{e}}_0 = \begin{bmatrix} \boldsymbol{x}_0 - \hat{\boldsymbol{x}}_0 \\ \boldsymbol{f}_0 - \hat{\boldsymbol{f}}_0 \end{bmatrix} \in \mathcal{X}_{\bar{e},0} = \langle \boldsymbol{0}, \quad \boldsymbol{G}_{\bar{e},0} \rangle = \langle \boldsymbol{0}, \begin{bmatrix} \boldsymbol{G}_{x,0} & \\ & \boldsymbol{G}_{f,0} \end{bmatrix} \rangle \tag{61}$$

Taking into account the augmented error dynamic system (35) and the observer (24), the augmented error $\bar{\boldsymbol{e}}_k$ can be contained by $\mathcal{X}_{\bar{e},k} = \langle \boldsymbol{0}, \boldsymbol{G}_{\bar{e},k} \rangle \in \mathbb{R}^{n_x + n_f}$. Then, the interval estimation $[\boldsymbol{x}_k]$ and $[\boldsymbol{f}_k]$ are determined as

$$\begin{cases} \boldsymbol{x}_k^-(i) = \hat{\boldsymbol{x}}_k(i) - \|\boldsymbol{G}_{\bar{e},k}(i,:)\|_1 \\ \boldsymbol{x}_k^+(i) = \hat{\boldsymbol{x}}_k(i) + \|\boldsymbol{G}_{\bar{e},k}(i,:)\|_1 \end{cases}, \tag{62}$$

$$\begin{cases} \boldsymbol{f}_k^-(j) = \hat{\boldsymbol{f}}_k(j) - \|\boldsymbol{G}_{\bar{e},k}(n_x + j,:)\|_1 \\ \boldsymbol{f}_k^+(j) = \hat{\boldsymbol{f}}_k(j) + \|\boldsymbol{G}_{\bar{e},k}(n_x + j,:)\|_1 \end{cases}, \tag{63}$$

$$i = 1, \ldots, n_x, \quad j = 1, \ldots, n_f.$$

where

$$\boldsymbol{G}_{\bar{e},k} = \downarrow_d (\tilde{\boldsymbol{G}}_{\bar{e},k}) \tag{64}$$

$$\tilde{\boldsymbol{G}}_{\bar{e},k} = [\boldsymbol{S}\boldsymbol{G}_{\bar{e},k-1} \quad \overline{\boldsymbol{T}}\tilde{\boldsymbol{G}}_{\boldsymbol{x},k-1} \quad \overline{\boldsymbol{E}}\boldsymbol{G}_{\overline{\boldsymbol{w}}}] \tag{65}$$

$$\tilde{\boldsymbol{G}}_{\boldsymbol{x},k-1} = \mathrm{ZonIn}([\boldsymbol{H}]_{k-1} \boldsymbol{G}_{\boldsymbol{x},k-1}) \tag{66}$$

$$\boldsymbol{G}_{\overline{\boldsymbol{w}}} = \mathrm{diag}([\tilde{\boldsymbol{w}} \quad \boldsymbol{\Delta}\tilde{\boldsymbol{f}} \quad \tilde{\boldsymbol{v}} \quad \tilde{\boldsymbol{v}}]^{\mathrm{T}}) \tag{67}$$

$$[\boldsymbol{H}]_{k-1} = [\frac{\partial \boldsymbol{h}}{\partial \boldsymbol{x}}]([\boldsymbol{x}_{k-1}^-, \boldsymbol{x}_{k-1}^+], \boldsymbol{u}_{k-1}) \tag{68}$$

$$\boldsymbol{G}_{\boldsymbol{x},k-1} = \boldsymbol{G}_{\bar{e},k-1}(1 : n_x, 1 : n_x) \tag{69}$$

Proof. Based on Assumption 3, (23) can be converted to the following zonotope form

$$\begin{aligned} &\boldsymbol{x}_0 \in \mathcal{X}_{\boldsymbol{x},0} = \langle \boldsymbol{c}_{x,0}, \boldsymbol{G}_{x,0} \rangle = \langle \boldsymbol{c}_{x,0}, \mathrm{diag}(\tilde{\boldsymbol{x}}) \rangle, \\ &\boldsymbol{f}_0 \in \mathcal{X}_{f,0} = \langle \boldsymbol{c}_{f,0}, \boldsymbol{G}_{f,0} \rangle = \langle \boldsymbol{c}_{f,0}, \mathrm{diag}(\tilde{\boldsymbol{f}}) \rangle. \end{aligned} \tag{70}$$

Given $\hat{\boldsymbol{x}}_0 = \boldsymbol{c}_{x,0}$ and $\hat{\boldsymbol{f}}_0 = \boldsymbol{c}_{f,0}$, the initial augmented error $\bar{\boldsymbol{e}}_0$ and disturbance $\overline{\boldsymbol{w}}_k$ is contained by

$$\begin{aligned} &\bar{\boldsymbol{e}}_0 \in \mathcal{X}_{\bar{e},0} = \langle \boldsymbol{0}, \boldsymbol{G}_{\bar{e},0} \rangle = \langle \boldsymbol{0}, \begin{bmatrix} \boldsymbol{G}_{x,0} & \\ & \boldsymbol{G}_{f,0} \end{bmatrix} \rangle, \\ &\overline{\boldsymbol{w}}_k \in \mathcal{X}_{\overline{\boldsymbol{w}}} = \langle \boldsymbol{0}, \boldsymbol{G}_{\overline{\boldsymbol{w}}} \rangle = \langle \boldsymbol{0}, \mathrm{diag}([\tilde{\boldsymbol{w}}^{\mathrm{T}} \ \boldsymbol{\Delta}\tilde{\boldsymbol{f}}^{\mathrm{T}} \ \tilde{\boldsymbol{v}}^{\mathrm{T}} \ \tilde{\boldsymbol{v}}^{\mathrm{T}}]^{\mathrm{T}}) \rangle. \end{aligned} \tag{71}$$

Correspondingly, we have

$$\begin{aligned} &\boldsymbol{x}_k \in \mathcal{X}_{\boldsymbol{x},k} = \langle \hat{\boldsymbol{x}}_k, \boldsymbol{G}_{x,k} \rangle, \boldsymbol{f}_k \in \mathcal{X}_{f,k} = \langle \hat{\boldsymbol{f}}_k, \boldsymbol{G}_{f,k} \rangle, \\ &\bar{\boldsymbol{e}}_k = \begin{bmatrix} \boldsymbol{x}_k - \hat{\boldsymbol{x}}_k \\ \boldsymbol{f}_k - \hat{\boldsymbol{f}}_k \end{bmatrix} \in \mathcal{X}_{\bar{e},k} = \langle \boldsymbol{0}, \boldsymbol{G}_{\bar{e},k} \rangle = \langle \boldsymbol{0}, \begin{bmatrix} \boldsymbol{G}_{x,k} & \\ & \boldsymbol{G}_{f,k} \end{bmatrix} \rangle. \end{aligned} \tag{72}$$

Then, according to the augmented error system (35), we obtain

$$\begin{aligned} \bar{\boldsymbol{e}}_k &= \boldsymbol{S}\bar{\boldsymbol{e}}_{k-1} + \overline{\boldsymbol{T}}\boldsymbol{\Delta h}_{k-1} + \overline{\boldsymbol{E}}\overline{\boldsymbol{w}}_{k-1} \\ &\in \boldsymbol{S}\mathcal{X}_{\bar{e},k-1} \oplus \overline{\boldsymbol{T}}(\boldsymbol{h}(\mathcal{X}_{\boldsymbol{x},k-1}, \boldsymbol{u}_k - 1) - \boldsymbol{h}(\hat{\boldsymbol{x}}_{k-1}, \boldsymbol{u}_{k-1})) \oplus \overline{\boldsymbol{E}}\mathcal{X}_{\overline{\boldsymbol{w}}}. \end{aligned} \tag{73}$$

Based on $\mathcal{X}_{\boldsymbol{x},k-1} = \langle \hat{\boldsymbol{x}}_{k-1}, \boldsymbol{G}_{\boldsymbol{x},k-1} \rangle$, Lemmas 4 and 5, it can be shown that

$$\begin{aligned} &\boldsymbol{h}(\mathcal{X}_{\boldsymbol{x},k-1}, \boldsymbol{u}_{k-1}) - \boldsymbol{h}(\hat{\boldsymbol{x}}_{k-1}, \boldsymbol{u}_{k-1}) \\ &\subseteq [\frac{\partial \boldsymbol{h}}{\partial \boldsymbol{x}}](\mathcal{X}_{\boldsymbol{x},k-1}, \boldsymbol{u}_{k-1})(\mathcal{X}_{\boldsymbol{x},k-1} - \hat{\boldsymbol{x}}_{k-1}) \\ &\subseteq [\frac{\partial \boldsymbol{h}}{\partial \boldsymbol{x}}]([\boldsymbol{x}_{k-1}], \boldsymbol{u}_{k-1}) \langle \boldsymbol{0}, \boldsymbol{G}_{\boldsymbol{x},k-1} \rangle \\ &\subseteq \langle \boldsymbol{0}, \mathrm{ZonIn}([\frac{\partial \boldsymbol{h}}{\partial \boldsymbol{x}}]([\boldsymbol{x}_{k-1}^-, \boldsymbol{x}_{k-1}^+], \boldsymbol{u}_{k-1}) \boldsymbol{G}_{\boldsymbol{x},k-1}) \rangle. \end{aligned} \tag{74}$$

Defining

$$[\boldsymbol{H}]_{k-1} = [\frac{\partial \boldsymbol{h}}{\partial \boldsymbol{x}}]([\boldsymbol{x}_{k-1}^-, \boldsymbol{x}_{k-1}^+], \boldsymbol{u}_{k-1}),$$

$$\tilde{\boldsymbol{G}}_{\boldsymbol{x},k-1} = \mathrm{ZonIn}([\boldsymbol{H}]_{k-1} \boldsymbol{G}_{\boldsymbol{x},k-1}),$$

(74) can be rewritten as

$$\boldsymbol{h}(\mathcal{X}_{\boldsymbol{x},k-1}, \boldsymbol{u}_{k-1}) - \boldsymbol{h}(\hat{\boldsymbol{x}}_{k-1}, \boldsymbol{u}_{k-1}) \subseteq \langle \boldsymbol{0}, \tilde{\boldsymbol{G}}_{\boldsymbol{x},k-1} \rangle \tag{75}$$

Substituting (72), (75) into (73) and using Property 1 lead to

$$\begin{aligned} \bar{\boldsymbol{e}}_k &\in \boldsymbol{S} \langle \boldsymbol{0}, \boldsymbol{G}_{\bar{e},k-1} \rangle \oplus \overline{\boldsymbol{T}} \langle \boldsymbol{0}, \tilde{\boldsymbol{G}}_{\boldsymbol{x},k-1} \rangle \oplus \overline{\boldsymbol{E}} \langle \boldsymbol{0}, \boldsymbol{G}_{\overline{\boldsymbol{w}}} \rangle \\ &= \langle \boldsymbol{0}, [\boldsymbol{S}\boldsymbol{G}_{\bar{e},k-1} \quad \overline{\boldsymbol{T}}\tilde{\boldsymbol{G}}_{\boldsymbol{x},k-1} \quad \overline{\boldsymbol{E}}\boldsymbol{G}_{\overline{\boldsymbol{w}}}] \rangle \\ &= \langle \boldsymbol{0}, \tilde{\boldsymbol{G}}_{\bar{e},k} \rangle \subseteq \langle \boldsymbol{0}, \downarrow_d (\tilde{\boldsymbol{G}}_{\bar{e},k}) \rangle = \langle \boldsymbol{0}, \boldsymbol{G}_{\bar{e},k} \rangle. \end{aligned} \tag{76}$$

which completes the proof. □

The proposed algorithm are summarized as follows:

Step 1. Off-line observer design:

(a) Set $\boldsymbol{\Theta}$ and then determine $\boldsymbol{T}$, $\boldsymbol{N}$ by using (28) and (29).

(b) Calculate matrices $\boldsymbol{H}_i$ (for $i, \ldots, \eta$) based on (58).

(c) Select bounds $\tilde{\boldsymbol{w}}$, $\tilde{\boldsymbol{v}}$, $\boldsymbol{\Delta}\tilde{\boldsymbol{f}}$ and then determine $\boldsymbol{L}_1$, $\boldsymbol{L}_2$ by solving (37) under constraints (39).

Step 2. On-line interval estimation:

(a) Select initial state $\boldsymbol{c}_{x,0}, \boldsymbol{c}_{f,0}$ and initial bounds $\tilde{\boldsymbol{x}}, \tilde{\boldsymbol{f}}$ to calculate initial zonotopes $\mathcal{X}_{x,0}, \mathcal{X}_{f,0}$. Then determine the bounds of state $[\boldsymbol{x}_k]$ and fault $[\boldsymbol{f}_k]$ by propagating (62)–(69).

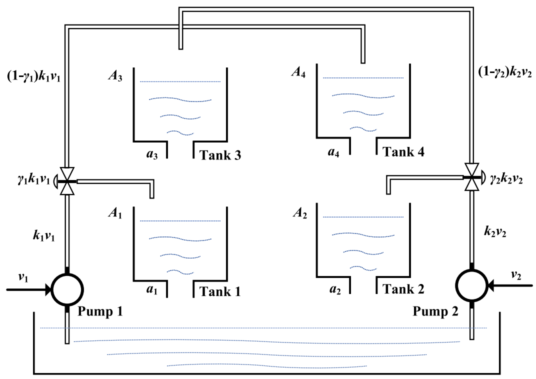

Fig. 1. The diagram of quadruple-tank system.

5. Simulations

In this section, a quadruple-tank system from [26] is used to demonstrate the effectiveness and superiority of the proposed interval estimation method. The diagram of quadruple-tank system is depicted in Fig. 1. The mathematical model of the quadruple-tanks system derived from Bernoulli′s theorem and mass balances can be described as

$$\begin{aligned}
\dot{h}_1(t) &= -\frac{a_1}{A_1}\sqrt{2\,gh_1(t)} + \frac{a_3}{A_1}\sqrt{2\,gh_3(t)} + \frac{\gamma_1 k_1}{A_1}v_1(t),\\
\dot{h}_2(t) &= -\frac{a_2}{A_2}\sqrt{2\,gh_2(t)} + \frac{a_4}{A_2}\sqrt{2\,gh_4(t)} + \frac{\gamma_2 k_2}{A_2}v_2(t),\\
\dot{h}_3(t) &= -\frac{a_3}{A_3}\sqrt{2\,gh_3(t)} + \frac{\left(1-\gamma_2\right)k_2}{A_3}v_2(t),\\
\dot{h}_4(t) &= -\frac{a_4}{A_4}\sqrt{2\,gh_4(t)} + \frac{\left(1-\gamma_1\right)k_1}{A_4}v_1(t).
\end{aligned} \tag{77}$$

where $t \in \mathbb{R}^{\geq 0}$ is time. The model parameters are shown in Table 1.

Defining $\boldsymbol{x} = [h_1(t) \quad h_2(t) \quad h_3(t) \quad h_4(t)]^{\mathrm{T}}$ and $\boldsymbol{u} = [v_1(t) \quad v_2(t)]^{\mathrm{T}}$, (77) can be rewritten as

$$\dot{\boldsymbol{x}} = \boldsymbol{A}_L(\boldsymbol{x})\boldsymbol{x} + \boldsymbol{B}\boldsymbol{u}, \tag{78}$$

with

$$\boldsymbol{A}_L(\boldsymbol{x}) = \begin{bmatrix} -\frac{a_1\sqrt{2g}}{A_1\sqrt{h_1}} & 0 & \frac{a_3\sqrt{2g}}{A_1\sqrt{h_3}} & 0 \\ 0 & -\frac{a_2\sqrt{2g}}{A_2\sqrt{h_2}} & 0 & \frac{a_4\sqrt{2g}}{A_2\sqrt{h_4}} \\ 0 & 0 & -\frac{a_3\sqrt{2g}}{A_3\sqrt{h_3}} & 0 \\ 0 & 0 & 0 & -\frac{a_4\sqrt{2g}}{A_4\sqrt{h_4}} \end{bmatrix},$$

$$\boldsymbol{B} = \begin{bmatrix} \frac{\gamma_1 k_1}{A_1} & 0 \\ 0 & \frac{\gamma_2 k_2}{A_2} \\ 0 & \frac{(1-\gamma_2)k_2}{A_3} \\ \frac{(1-\gamma_1)k_1}{A_4} & 0 \end{bmatrix} = \begin{bmatrix} 0.0653 & 0 \\ 0 & 0.0488 \\ 0 & 0.0628 \\ 0.0440 & 0 \end{bmatrix}.$$

For $\boldsymbol{u} = [10 \quad 10]^{\mathrm{T}}$ and based on (77), the equilibrium point $\boldsymbol{x}_e$ can be calculated $\boldsymbol{x}_e = [130.1 \quad 172.6 \quad 31.3 \quad 38.8]^{\mathrm{T}}$. Expanding (77) around the equilibrium point $\boldsymbol{x}_e$ and discretizing it with $T_s = 1$s using Euler method, we obtain

$$\begin{aligned}
\boldsymbol{x}_{k+1} &= (\boldsymbol{I}_{n_x} + \boldsymbol{A}_L(\boldsymbol{x}_e))\boldsymbol{x}_k + \boldsymbol{B}\boldsymbol{u}_k + (\boldsymbol{A}_L(\boldsymbol{x}_k) - \boldsymbol{A}_L(\boldsymbol{x}_e))\boldsymbol{x}_k \\
&= \boldsymbol{A}\boldsymbol{x}_k + \boldsymbol{B}\boldsymbol{u}_k + \boldsymbol{h}(\boldsymbol{x}_k, \boldsymbol{u}_k)
\end{aligned} \tag{79}$$

Considering actuator fault, unknown input, process disturbance, and measurement noise, (79) can be expressed as the form of (16) as follows:

$$\begin{cases} \boldsymbol{x}_{k+1} = \boldsymbol{A}\boldsymbol{x}_k + \boldsymbol{B}\boldsymbol{u}_k + \boldsymbol{D}\boldsymbol{d}_k + \boldsymbol{h}(\boldsymbol{x}_k, \boldsymbol{u}_k) + \boldsymbol{B}\boldsymbol{f}_k + \boldsymbol{E}_1\boldsymbol{w}_k, \\ \boldsymbol{y}_k = \boldsymbol{C}\boldsymbol{x}_k + \boldsymbol{E}_2\boldsymbol{v}_k. \end{cases} \tag{80}$$

Table 1
The model parameters of quadruple-tank system.

Symbol	Definition and value
$h_i(t)$	The ith tank water level at the time t
$v_i(t)$	The ith pump input voltage at the time t
A_i	The ith tank cross-section: $A_1 = A_3 = 28$ cm^2, $A_2 = A_4 = 32$ cm^2
a_i	The ith outlet hole cross-section: $a_1 = a_3 = 0.071$ cm^2, $a_2 = a_4 = 0.051$ cm^2
g	The gravity acceleration: $g = 9.8$ m/s^2
γ_i	The ith valve proportional coefficient: $\gamma_1 = 0.565$, $\gamma_2 = 0.47$
k_i	The ith pump proportional coefficient: $k_1 = 3.235$ cm^3/V s, $k_2 = 3.320$ cm^3/V s

with

$$\boldsymbol{A} = \begin{bmatrix} 0.9902 & 0 & 0.0201 & 0 \\ 0 & 0.9946 & 0 & 0.0113 \\ 0 & 0 & 0.9799 & 0 \\ 0 & 0 & 0 & 0.9887 \end{bmatrix}, \boldsymbol{D} = \begin{bmatrix} 0 \\ 0 \\ 1 \\ 0 \end{bmatrix},$$

$$\boldsymbol{C} = \begin{bmatrix} 1 & 0 & 0 & 0 \\ 0 & 1 & 0 & 0 \\ 0 & 0 & 1 & 0 \end{bmatrix}, \boldsymbol{E}_1 = \begin{bmatrix} 0.1 \\ 0.1 \\ 0.1 \\ 0.1 \end{bmatrix}, \boldsymbol{E}_2 = \begin{bmatrix} 1 \\ 1 \\ 1 \\ 1 \end{bmatrix}.$$

$$\boldsymbol{h}(\boldsymbol{x}_k, \boldsymbol{u}_k) = \begin{bmatrix} \rho_{11} & 0 & \rho_{13} & 0 \\ 0 & \rho_{22} & 0 & \rho_{24} \\ 0 & 0 & \rho_{33} & 0 \\ 0 & 0 & 0 & \rho_{44} \end{bmatrix}\begin{bmatrix} h_1 \\ h_2 \\ h_3 \\ h_4 \end{bmatrix},$$

$$\rho_{11} = -\frac{0.11235}{\sqrt{h_1}} - 0.9902, \rho_{13} = \frac{0.11235}{\sqrt{h_3}} - 0.0201,$$

$$\rho_{22} = -\frac{0.07059}{\sqrt{h_2}} - 0.9946, \rho_{24} = \frac{0.07059}{\sqrt{h_4}} - 0.0113,$$

$$\rho_{33} = -\frac{0.11235}{\sqrt{h_3}} - 0.9799, \rho_{44} = -\frac{0.07059}{\sqrt{h_4}} - 0.9887.$$

In this paper, the water level of tanks is assumed to be $h_1, h_2 \in [60, 280]$ and $h_3, h_4 \in [5, 100]$, that is $\boldsymbol{x}^- = [60 \quad 60 \quad 5 \quad 5]^{\mathrm{T}}$ and $\boldsymbol{x}^+ = [280 \quad 280 \quad 100 \quad 100]^{\mathrm{T}}$. Based on (18), the bounds of $[\boldsymbol{H}] = [\boldsymbol{H}^-, \boldsymbol{H}^+]$ can be obtained as

$$\boldsymbol{H}^- = \begin{bmatrix} 0.0026 & 0 & -0.0145 & 0 \\ 0 & 0.0008 & 0 & -0.0078 \\ 0 & 0 & -0.005 & 0 \\ 0 & 0 & 0 & -0.0045 \end{bmatrix},$$

$$\boldsymbol{H}^+ = \begin{bmatrix} 0.0065 & 0 & 0.005 & 0 \\ 0 & 0.0033 & 0 & 0.0045 \\ 0 & 0 & 0.0145 & 0 \\ 0 & 0 & 0 & 0.0078 \end{bmatrix}.$$

with the form of $\frac{\partial h}{\partial x}(\boldsymbol{x}, \boldsymbol{u})$ is given in Appendix. Then, the matrix $\boldsymbol{H}_i$ has $\eta = 2^{4^2-10} = 64$ vertices.

In the simulations, the initial state value and the input voltage of pumps are chosen as $\boldsymbol{x}_0 = [130 \quad 170 \quad 30 \quad 40]^{\mathrm{T}}$ and $\boldsymbol{u}_k = [10 + \sin(k/50) \quad 10 + \cos(k/80)]^{\mathrm{T}}$, respectively. The constant input disturbance is set as $\boldsymbol{d}_k = 1$. The process disturbance $\boldsymbol{w}_k \in [-0.1, 0.1]$ and measurement noise $\boldsymbol{v}_k \in [-0.1, 0.1]$ are considered, which yields that $\tilde{\boldsymbol{w}} = 0.1$ and $\tilde{\boldsymbol{v}} = 0.1$. The initial state of interval observer are set as $\hat{\boldsymbol{x}}_0 = \boldsymbol{c}_{x,0} = [125 \quad 165 \quad 25 \quad 35]^{\mathrm{T}}$, $\hat{\boldsymbol{f}}_0 = \boldsymbol{c}_{f,0} = [0 \quad 0]^{\mathrm{T}}$. Moreover, the initial bounds of state and fault are chosen as $\tilde{\boldsymbol{x}} = [5 \quad 5 \quad 5 \quad 5]^{\mathrm{T}}$ and $\tilde{\boldsymbol{f}} = [5 \quad 5]^{\mathrm{T}}$. The integer of zonotope reduce operator and the bound of actuator fault variation are set as $d = 50$ and $\Delta\tilde{\boldsymbol{f}} = 0.05$, respectively.

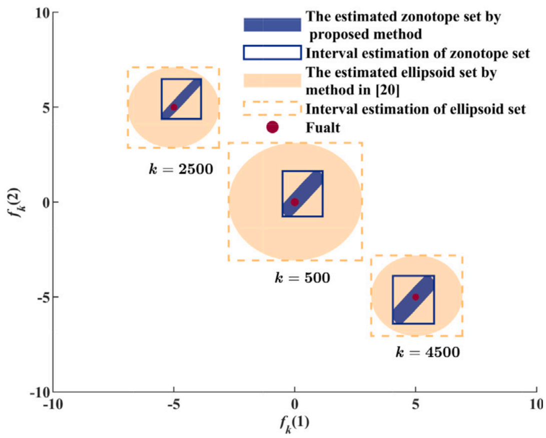

Fig. 2. f_k, estimated set and interval estimation under fault scenario 1 at $k = 500, 2500, 4500$.

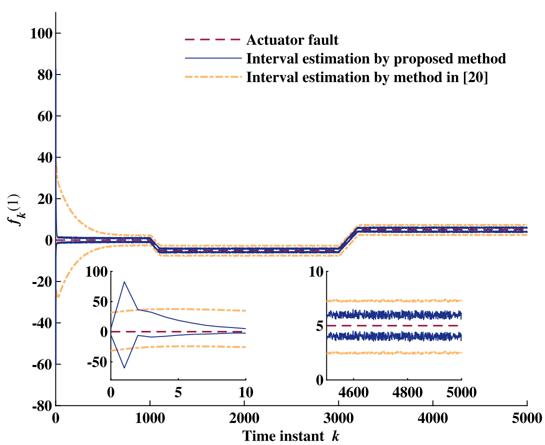

Fig. 3. $f_k(1)$ and interval estimation under fault scenario 1.

Considering (28)–(29), we have

$$\boldsymbol{\Theta} = \begin{bmatrix} 0 & 0 & 0 \\ 0.5 & 0 & 0 \\ 0 & 0 & 0 \\ 0 & 0 & 0 \end{bmatrix}, \boldsymbol{T} = \begin{bmatrix} 1 & 0 & 0 & 0 \\ -0.5 & 1 & 0 & 0 \\ 0 & 0 & 0 & 0 \\ 0 & 0 & 0 & 1 \end{bmatrix},$$

$$\boldsymbol{N} = \begin{bmatrix} 0 & 0 & 0 \\ 0.5 & 0 & 0 \\ 0 & 0 & 1 \\ 0 & 0 & 0 \end{bmatrix}$$

Then, solving the optimization problem (60) (for $i = 1, \ldots, \eta$), we obtain

$$\boldsymbol{L}_1 = \begin{bmatrix} 1.3384 & -0.3653 & -0.3079 \\ -0.7175 & 1.6388 & -0.5897 \\ -0.0016 & -0.0008 & 0.0012 \\ 0.8490 & -0.3787 & -0.0785 \end{bmatrix},$$

$$\boldsymbol{L}_2 = \begin{bmatrix} 6.4207 & -5.6908 & 1.1436 \\ 0.1995 & 9.5112 & -7.1120 \end{bmatrix}$$

with H_∞ performance index $\delta = 5.0381$.

The following fault scenarios affecting the pumps are defined as follows:

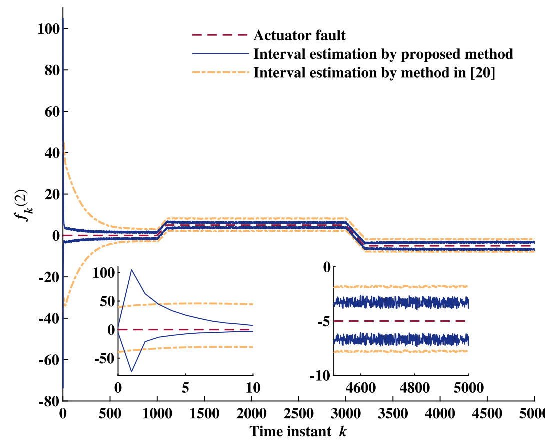

Fig. 4. $f_k(2)$ and interval estimation under fault scenario 1.

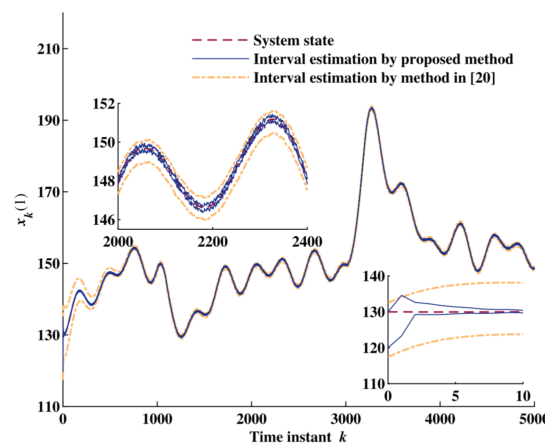

Fig. 5. $x_k(1)$ and interval estimation under fault scenario 1.

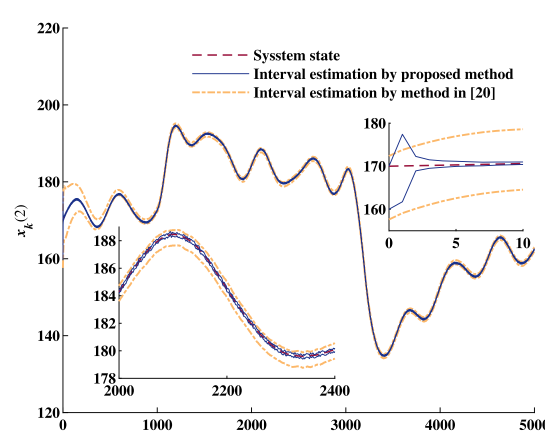

Fig. 6. $x_k(2)$ and interval estimation under fault scenario 1.

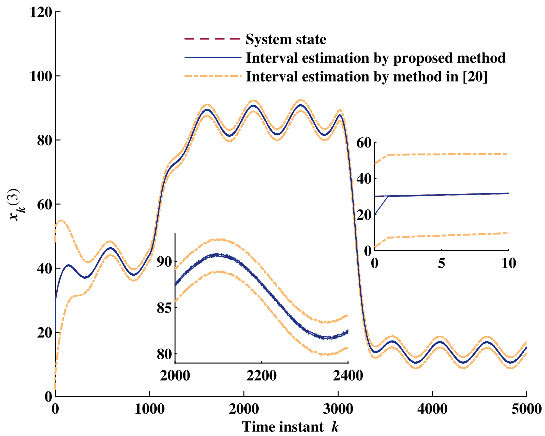

Fig. 7. $x_k(3)$ and interval estimation under fault scenario 1.

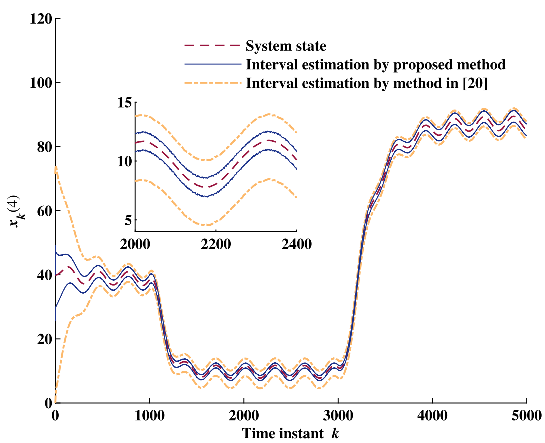

Fig. 8. $x_k(4)$ and interval estimation under fault scenario 1.

-Fault scenario 1:

$$f_k(1) = \begin{cases} 0 & 0 \le k \le 1000 \\ -0.05k + 50 & 1000 < k \le 1100 \\ -5 & 1100 < k \le 3000 \\ 0.05k - 155 & 3000 < k \le 3200 \\ 5 & 3200 < k \le 5000. \end{cases}$$

$$f_k(2) = \begin{cases} 0 & 0 \le k \le 1000 \\ 0.05k - 50 & 1000 < k \le 1100 \\ 5 & 1100 < k \le 3000 \\ -0.05k + 155 & 3000 < k \le 3200 \\ -5 & 3200 < k \le 5000. \end{cases}$$

-Fault scenario 2:

$$f_k(1) = \begin{cases} 0 & 0 \le k \le 1000 \\ 5\sin(0.005k - 1) & 1000 < k \le 5000. \end{cases}$$

$$f_k(2) = \begin{cases} 0 & 0 \le k \le 1000 \\ -5\sin(0.005k - 1) & 1000 < k \le 5000. \end{cases}$$

Interval estimation of actuator fault and state based on the proposed method is compared with a bounded-error approach [26]. The parameters of the bounded-error approach are detailed in Appendix. Figs. 2 and 9 demonstrate the actuator fault f_k, its estimated set, and its interval estimation based on proposed method and method in [26] under two fault scenarios at $k = 500, 2500, 4500$. Under fault scenario 1, the interval estimation results are presented in Figs. 3–8. Similarly, for fault scenario 2, the estimation results are shown in Figs. 10–15. In Figs. 3–8 and 10–15, the dashed line, the solid line, and the dash-dotted line stand for actuator fault/states, interval estimation based on the proposed method and interval estimation based on the bounded-error approach [26], respectively. In these figures, the proposed method achieves interval estimation convergence within approximately 10 steps, whereas the method presented in [26] necessitates 500 steps for convergence. Additionally, we compare the interval widths between the two methods. The interval width can be calculated as the difference between the upper and lower bounds: $f_k^+ - f_k^-$ and $x_k^+ - x_k^-$. Then, the average widths of interval estimation under two fault scenarios obtained by the applied two methods are shown in Tables 2 and 3. Comparative analysis of simulation results reveals that the proposed method outperforms the existing approach [26]. Specifically, it demonstrates faster convergence and a tighter estimation interval. Furthermore, even in scenarios involving multiple faults, our method effectively handles the fault and state estimation.

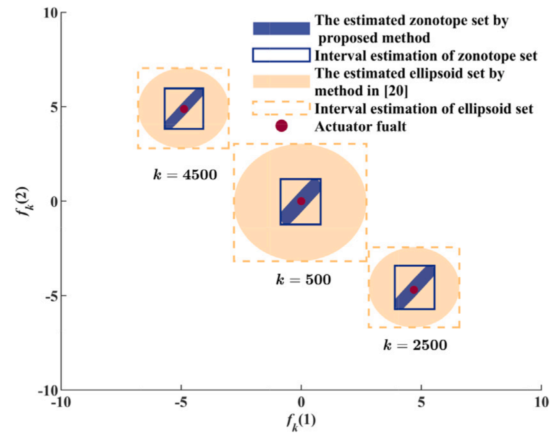

Fig. 9. f_k, estimated set and interval estimation under fault scenario 2 at $k = 500, 2500, 4500$.

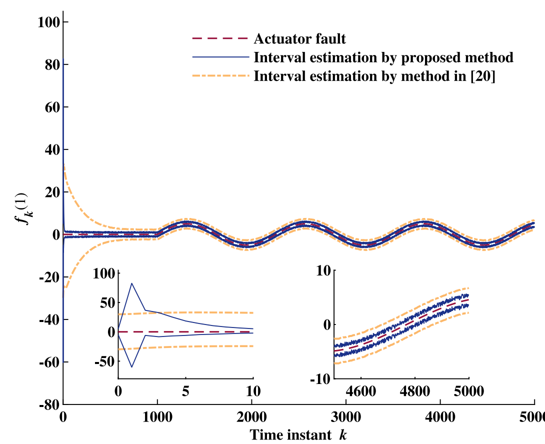

Fig. 10. $f_k(1)$ and interval estimation under fault scenario 2.

Remark 3. Based on the H_∞ design condition, the proposed method has good robustness to nonlinear systems subjected to multiple process disturbances and measurement noise. Moreover, the T–N–L observer can also decouple the influence of unknown inputs, which are widely present in real world. A highly coupled nonlinear system can be transformed into the system considered in this paper by using the equilibrium point linearization method. It is worth noting that when the system state is far from the chosen equilibrium point, the equilibrium point linearization method may not be the optimal choice. Therefore, selecting an appropriate linearization method for different nonlinear systems will be the focus of our future research.

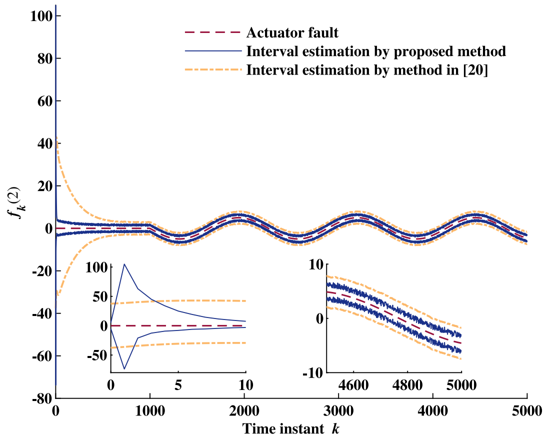

Fig. 11. $f_k(2)$ and interval estimation under fault scenario 2.

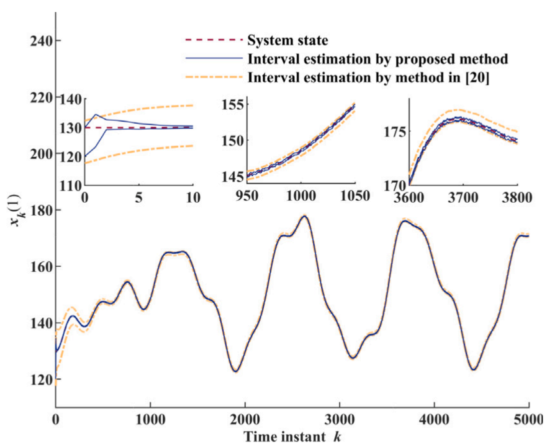

Fig. 12. $x_k(1)$ and interval estimation under fault scenario 2.

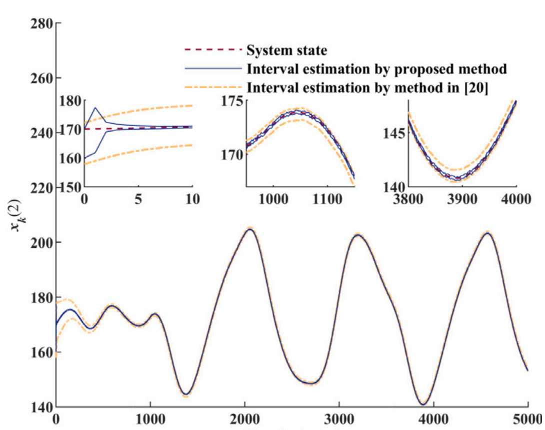

Fig. 13. $x_k(2)$ and interval estimation under fault scenario 2.

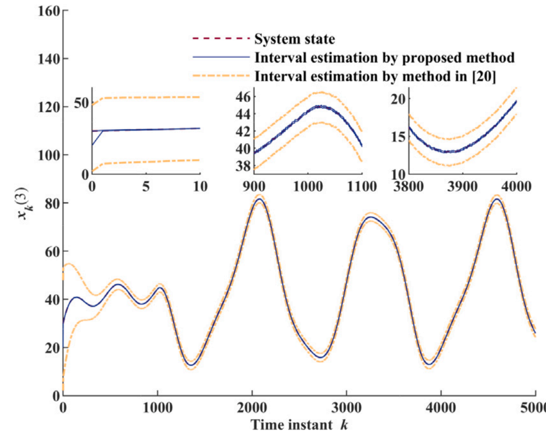

Fig. 14. $x_k(3)$ and interval estimation under fault scenario 2.

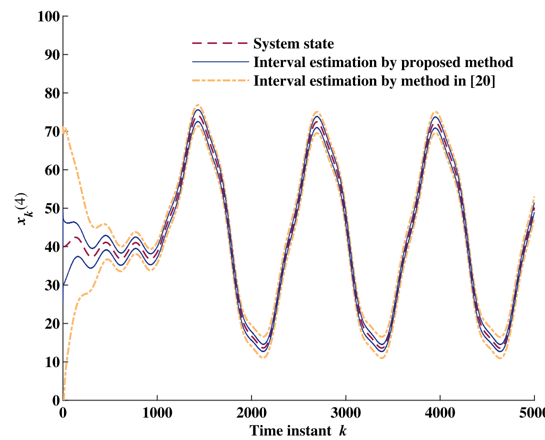

Fig. 15. $x_k(4)$ and interval estimation under fault scenario 2.

Table 2
The average width of interval estimation during $0 \le k \le 5000$ for fault scenario 1.

Method	$f_k(1)$	$f_k(2)$	$x_k(1)$	$x_k(2)$	$x_k(3)$	$x_k(4)$
The method in [26]	6.76	8.40	1.61	1.58	4.92	7.76
The proposed method	1.93	3.11	0.30	0.28	0.20	2.97

Table 3
The average width of interval estimation during $0 \le k \le 5000$ for fault scenario 2.

Method	$f_k(1)$	$f_k(2)$	$x_k(1)$	$x_k(2)$	$x_k(3)$	$x_k(4)$
The method in [26]	6.76	8.40	1.61	1.58	4.92	7.76
The proposed method	1.94	3.17	0.31	0.29	0.20	3.11

6. Conclusions

In this paper, the simultaneous actuator fault and state interval estimation problem for a class of nonlinear systems affected by unknown but bounded disturbances and noise has been investigated. These systems satisfy both a one-sided Lipschitz condition and a standard Lipschitz condition. The proposed T–N–L observer not only employs H_∞ method to attenuate the effect of unknown but peak bounded process disturbances and measurement noise present in real-world, but also can decouple the effect of unknown inputs. The simulations for a quadruple-tank system under different fault scenarios are conducted to show the superiority and effectiveness of the presented method. Moreover, a tighter actuator fault and state interval estimation method is achieved based on zonotope analysis compared to the existing method [26]. In the future, we plan to extend the proposed fault estimation method to Takagi–Sugeno fuzzy nonlinear systems and nonlinear systems described by state-space neural networks.

CRediT authorship contribution statement

Chi Xu: Writing – original draft. **Zhenhua Wang:** Writing – review & editing. **Vicenç Puig:** Writing – review & editing. **Yi Shen:** Writing – review & editing.

Declaration of competing interest

The authors declare the following financial interests/personal relationships which may be considered as potential competing interests: Zhenhua Wang reports financial support was provided by National Natural Science Foundation of China. If there are other authors, they declare that they have no known competing financial interests or personal relationships that could have appeared to influence the work reported in this paper.

Data availability

The authors do not have permission to share data.

Appendix. The calculation of interval matrix $[\boldsymbol{H}]$

The form of $\frac{\partial \boldsymbol{h}}{\partial \boldsymbol{x}}(\boldsymbol{x},\boldsymbol{u})$ is given as follows:

$$\frac{\partial \boldsymbol{h}}{\partial \boldsymbol{x}}(\boldsymbol{x},\boldsymbol{u}) = \begin{bmatrix} \bar{\rho}_{11} & 0 & \bar{\rho}_{13} & 0 \\ 0 & \bar{\rho}_{22} & 0 & \bar{\rho}_{24} \\ 0 & 0 & \bar{\rho}_{33} & 0 \\ 0 & 0 & 0 & \bar{\rho}_{44} \end{bmatrix} \tag{A.1}$$

where

$$\bar{\rho}_{11} = 0.009847 - \frac{0.0562}{\sqrt{\boldsymbol{x}(1)}}, \bar{\rho}_{13} = \frac{0.0562}{\sqrt{\boldsymbol{x}(3)}} - 0.0201$$
$$\bar{\rho}_{22} = 0.00537 - \frac{0.0353}{\sqrt{\boldsymbol{x}(2)}}, \bar{\rho}_{24} = \frac{0.0353}{\sqrt{\boldsymbol{x}(4)}} - 0.0113$$
$$\bar{\rho}_{33} = 0.0201 - \frac{0.0562}{\sqrt{\boldsymbol{x}(3)}}, \bar{\rho}_{44} = 0.0113 - \frac{0.0353}{\sqrt{\boldsymbol{x}(4)}}$$

Based on the $[\boldsymbol{x}] = [\boldsymbol{x}^-, \boldsymbol{x}^+]$ and (A.1), the $[\boldsymbol{H}] = [\boldsymbol{H}^-, \boldsymbol{H}^+]$ can be calculated.

A.1. The bounded-error approach

The structure of actuator fault and state estimator in [26] is as follows:

$$\begin{cases} \boldsymbol{z}_{k+1} = \boldsymbol{N}\boldsymbol{z}_k + \boldsymbol{G}\boldsymbol{u}_k + \boldsymbol{L}\boldsymbol{y}_k + \boldsymbol{T}\boldsymbol{B}\hat{\boldsymbol{f}}_k + \boldsymbol{T}\boldsymbol{h}(\hat{\boldsymbol{x}}_k, \boldsymbol{u}_k), \\ \hat{\boldsymbol{x}}_k = \boldsymbol{z}_k - \boldsymbol{E}\boldsymbol{y}_k, \\ \hat{\boldsymbol{f}}_{k+1} = \hat{\boldsymbol{f}}_k + \boldsymbol{F}(\boldsymbol{y}_k - \boldsymbol{C}\hat{\boldsymbol{x}}_k), \end{cases} \tag{A.2}$$

where

$$\boldsymbol{T} = \boldsymbol{I} + \boldsymbol{E}\boldsymbol{C}, \boldsymbol{G} = \boldsymbol{T}\boldsymbol{B}, \boldsymbol{K} = \boldsymbol{N}\boldsymbol{E} + \boldsymbol{L}, \boldsymbol{N} = \boldsymbol{T}\boldsymbol{A} - \boldsymbol{K}\boldsymbol{C}.$$

Under Assumption 3, it can be obtained

$$\boldsymbol{E} = -\boldsymbol{D}[(\boldsymbol{C}\boldsymbol{D})^{\mathrm{T}}(\boldsymbol{C}\boldsymbol{D})]^{-1}(\boldsymbol{C}\boldsymbol{D})^{\mathrm{T}} \tag{A.3}$$

The bound of the actuator fault and state estimator can be calculated as follows:

$$\begin{cases} \boldsymbol{x}_k^-(i) = \hat{\boldsymbol{x}}_k(i) - \boldsymbol{b}_k(i) \\ \boldsymbol{x}_k^+(i) = \hat{\boldsymbol{x}}_k(i) - \boldsymbol{b}_k(i) \end{cases}, \quad i = 1, \dots, n_x$$
$$\begin{cases} \boldsymbol{f}_k^-(j) = \hat{\boldsymbol{f}}_k(j) - \boldsymbol{b}_k(i) \\ \boldsymbol{f}_k^+(j) = \hat{\boldsymbol{f}}_k(j) - \boldsymbol{b}_k(i) \end{cases}, \tag{A.4}$$
$$j = 1, \dots, n_y, \quad i = n_x + 1, \dots, n_x + n_f$$

with

$$\boldsymbol{b}_k(i) = \sqrt{\zeta_k(\gamma)\boldsymbol{c}_i^{\mathrm{T}}\boldsymbol{P}^{-1}\boldsymbol{c}_i}, \tag{A.5}$$

$$\zeta_k(\gamma) = (1-\gamma)^k(V_0 - 1) + 1, \quad k = 0, 1, \dots \tag{A.6}$$

$$V_0 = \bar{\boldsymbol{e}}_0^{\mathrm{T}}\boldsymbol{P}\bar{\boldsymbol{e}}_0, \ \bar{\boldsymbol{e}}_0 = \begin{bmatrix} \boldsymbol{x}_0 - \hat{\boldsymbol{x}}_0 & \boldsymbol{f}_0 - \hat{\boldsymbol{f}}_0 \end{bmatrix}^{\mathrm{T}}, \tag{A.7}$$

where $\boldsymbol{c}_i$ is the ith column of an $n_x + n_f$ order identity matrix. With $\gamma = 0.01$, the following matrices can be obtained by solving LMI as follows

$$\boldsymbol{N} = \begin{bmatrix} 0.6315 & 0.0275 & 0.0793 & 0 \\ 0.0262 & 0.7383 & -0.0053 & 0.0113 \\ -8.6\times10^{-6} & -2.1\times10^{-6} & 4.8\times10^{-5} & 0 \\ -0.2542 & 0.0278 & 0.0511 & 0.9887 \end{bmatrix},$$

$$\boldsymbol{G} = \begin{bmatrix} 0.0653 & 0 \\ 0 & 0.0488 \\ 0 & 0 \\ 0.0440 & 0 \end{bmatrix}, \boldsymbol{T} = \begin{bmatrix} 1 & 0 & 0 & 0 \\ 0 & 1 & 0 & 0 \\ 0 & 0 & 0 & 0 \\ 0 & 0 & 0 & 1 \end{bmatrix},$$

$$\boldsymbol{E} = \begin{bmatrix} 0 & 0 & 0 \\ 0 & 0 & 0 \\ 0 & 0 & -1 \\ 0 & 0 & 0 \end{bmatrix}, \boldsymbol{F}^{\mathrm{T}} = \begin{bmatrix} 0.6107 & -0.0632 \\ -0.0306 & 0.5335 \\ -0.1255 & 0.0129 \end{bmatrix},$$

$$\boldsymbol{L} = \begin{bmatrix} 0.3587 & -0.0275 & 0.0201 \\ -0.0262 & 0.2563 & 0 \\ 8.6\times10^{-6} & 2.1\times10^{-6} & 0 \\ 0.2542 & -0.0278 & 0 \end{bmatrix},$$

$$\boldsymbol{P} = \begin{bmatrix} 10.6062 & -7.5802 & 0.0017 & 0.0825 & -0.7836 & 0.1131 \\ -7.5802 & 11.0193 & 0.0017 & -0.0816 & 0.2039 & -0.6611 \\ 0.0017 & 0.0017 & 0.3279 & 0.0000 & 0.0003 & 0.0003 \\ 0.0825 & -0.0816 & 0.0000 & 0.1099 & -0.0091 & 0.0651 \\ -0.7836 & 0.2039 & 0.0003 & -0.0091 & 0.2814 & -0.0024 \\ 0.1131 & -0.6611 & 0.0003 & 0.0651 & -0.0024 & 0.2226 \end{bmatrix}.$$

References

[1] F. Nemati, S.M.S. Hamami, A. Zemouche, A nonlinear observer-based approach to fault detection, isolation and estimation for satellite formation flight application, Automatica 107 (2019) 474–482.

[2] F. Xu, Observer-based asymptotic active fault diagnosis: A two-layer optimization framework, Automatica 128 (2021) 109558.

[3] Z. Wang, Y. Shen, Model-Based Fault Diagnosis: Methods for State-Space Systems, Springer Nature, 2023.

[4] M.A. Márquez-Vera, L. Ramos-Velasco, O. López-Ortega, N. Zúñiga-Peña, J. Ramos-Fernández, R.M. Ortega-Mendoza, Inverse fuzzy fault model for fault detection and isolation with least angle regression for variable selection, Comput. Ind. Eng. 159 (2021) 107499.

[5] B. Wang, Y. Shen, Y. Zhang, Active fault-tolerant control for a quadrotor helicopter against actuator faults and model uncertainties, Aerosp. Sci. Technol. 99 (2020) 105745.

[6] M. Hashemi, C.P. Tan, Integrated fault estimation and fault tolerant control for systems with generalized sector input nonlinearity, Automatica 119 (2020) 109098.

[7] F. Li, D. Kenan, S. Xu, C. Yi, K. Zhang, Iterative fault estimation and fault-tolerant control for a class of nonlinear variant time-delay systems, Internat. J. Robust Nonlinear Control 32 (15) (2022) 8486–8506.

[8] K. Ahmadi, D. Asadi, A. Merheb, S.-Y. Nabavi-Chashmi, O. Tutsoy, Active fault-tolerant control of quadrotor UAVs with nonlinear observer-based sliding mode control validated through hardware in the loop experiments, Control Eng. Pract. 137 (2023) 105557.

[9] Z. Gao, S.X. Ding, Actuator fault robust estimation and fault-tolerant control for a class of nonlinear descriptor systems, Automatica 43 (5) (2007) 912–920.

[10] J. Hu, Z. Wang, H. Gao, Joint state and fault estimation for time-varying nonlinear systems with randomly occurring faults and sensor saturations, Automatica 97 (2018) 150–160.

[11] W.-S. Chua, J.C.L. Chan, C.P. Tan, E.K.P. Chong, S. Saha, Robust fault reconstruction for a class of nonlinear systems, Automatica 113 (2020) 108718.

[12] J.-W. Zhu, G.-H. Yang, H. Wang, F. Wang, Fault estimation for a class of nonlinear systems based on intermediate estimator, IEEE Trans. Autom. Control 61 (9) (2015) 2518–2524.

[13] H. Kazemi, A. Yazdizadeh, Optimal state estimation and fault diagnosis for a class of nonlinear systems, IEEE/CAA J. Autom. Sin. 7 (2) (2020) 517–526.

[14] M. Witczak, M. Buciakowski, V. Puig, D. Rotondo, F. Nejjari, An LMI approach to robust fault estimation for a class of nonlinear systems, Internat. J. Robust Nonlinear Control 26 (7) (2016) 1530–1548.

[15] Y. Wu, D. Du, B. Liu, Z. Mao, Actuator fault estimation for two-stage chemical reactor system based on delta operator approach, J. Process Control 107 (2021) 37–46.
[16] S. Fu, J. Qiu, L. Chen, M. Chadli, Adaptive fuzzy observer-based fault estimation for a class of nonlinear stochastic hybrid systems, IEEE Trans. Fuzzy Syst. 30 (1) (2020) 39–51.
[17] W. Zhang, Z. Wang, Y. Shen, S. Guo, F. Zhu, Interval estimation of actuator fault by interval analysis, IET Control Theory Appl. 13 (16) (2019) 2717–2724.
[18] T. Chevet, A. Rauh, T.N. Dinh, J. Marzat, T. Raissi, Robust interval observer for systems described by the Fornasini–Marchesini second model, IEEE Control Syst. Lett. 6 (2021) 1940–1945.
[19] G. Marouani, T.N. Dinh, T. Raissi, X. Wang, H. Messaoud, Unknown input interval observers for discrete-time linear switched systems, Eur. J. Control 59 (2021) 165–174.
[20] T. Chevet, T.N. Dinh, J. Marzat, T. Raïssi, Robust sensor fault detection for linear parameter-varying systems using interval observer, in: 31st European Safety and Reliability Conference, 2021, pp. 1486–1493.
[21] Z. Wang, C.-C. Lim, Y. Shen, Interval observer design for uncertain discrete-time linear systems, Systems Control Lett. 116 (2018) 41–46.
[22] E.-J. Pérez-Pérez, J.-A. Fragoso-Mandujano, J.-A. Guzmán-Rabasa, Y. González-Baldizón, S.-K. Flores-Guirao, ANFIS and Takagi–Sugeno interval observers for fault diagnosis in bioprocess system, J. Process Control 138 (2024) 103225.
[23] W. Tang, Z. Wang, Y. Shen, Interval estimation for discrete-time linear systems: A two-step method, Systems Control Lett. 123 (2019) 69–74.
[24] W. Tang, Z. Wang, Q. Zhang, Y. Shen, Set-membership estimation for linear time-varying descriptor systems, Automatica 115 (2020) 108867.
[25] W. Zhang, Z. Wang, T. Raïssi, Y. Shen, Ellipsoid-based interval estimation for Lipschitz nonlinear systems, IEEE Trans. Autom. Control 67 (12) (2021) 6802–6809.
[26] M. Buciakowski, M. Witczak, V. Puig, D. Rotondo, F. Nejjari, J. Korbicz, A bounded-error approach to simultaneous state and actuator fault estimation for a class of nonlinear systems, J. Process Control 52 (2017) 14–25.
[27] W. Zhang, Z. Wang, T. Raïssi, R. Su, An ellipsoid-based framework for fault estimation and remaining useful life prognosis, Internat. J. Robust Nonlinear Control 33 (12) (2023) 7260–7281.
[28] Y. Wang, V. Puig, G. Cembrano, Robust fault estimation based on zonotopic Kalman filter for discrete-time descriptor systems, Internat. J. Robust Nonlinear Control 28 (16) (2018) 5071–5086.
[29] Y. Wang, Z. Wang, V. Puig, G. Cembrano, Zonotopic set-membership state estimation for discrete-time descriptor LPV systems, IEEE Trans. Autom. Control 64 (5) (2018) 2092–2099.
[30] M. Pourasghar, C. Combastel, V. Puig, C. Ocampo-Martinez, FD-ZKF: A zonotopic Kalman filter optimizing fault detection rather than state estimation, J. Process Control 73 (2019) 89–102.
[31] W. Zhang, Z. Wang, S. Guo, Y. Shen, Interval estimation of sensor fault based on zonotopic Kalman filter, Internat. J. Control 94 (6) (2021) 1641–1650.
[32] A.A. de Paula, G.V. Raffo, B.O. Teixeira, Zonotopic filtering for uncertain nonlinear systems: Fundamentals, implementation aspects, and extensions [applications of control], IEEE Control Syst. Mag. 42 (1) (2022) 19–51.
[33] A. Zemouche, M. Boutayeb, G.I. Bara, Observers for a class of Lipschitz systems with extension to H_∞ performance analysis, Systems Control Lett. 57 (1) (2008) 18–27.
[34] M.C. De Oliveira, J. Bernussou, J.C. Geromel, A new discrete-time robust stability condition, Systems Control Lett. 37 (4) (1999) 261–265.
[35] T. Alamo, J.M. Bravo, E.F. Camacho, Guaranteed state estimation by zonotopes, Automatica 41 (6) (2005) 1035–1043.
[36] L. Jaulin, M. Kieffer, O. Didrit, E. Walter, L. Jaulin, M. Kieffer, O. Didrit, É. Walter, Interval Analysis, Springer, 2001.
[37] M. Althoff, D. Grebenyuk, Implementation of interval arithmetic in CORA 2016, in: Proc. of the 3rd International Workshop on Applied Verification for Continuous and Hybrid Systems, 2016, pp. 91–105.
[38] S.P. Boyd, L. Vandenberghe, Convex Optimization, Cambridge University Press, 2004.